Chapter 5

Multiple Effect Evaporation Vapor Compression

Objectives

The objective of this chapter is to analyze and evaluate the performance of the multiple effect evaporation systems combined with various types of heat pumps. The analysis includes performance of the following systems:

- Parallel feed multiple effect evaporation with thermal or mechanical vapor compression heat pumps.
- Forward feed multiple effect evaporation with thermal, mechanical, absorption, or adsorption vapor compression heat pumps.

The performance of the parallel feed systems is compared against industrial data. However, the forward feed system presents only results of the system design, since there are no industrial units for these systems.

5.1 Parallel Feed Multiple Effect Evaporation with thermal and mechanical vapor compression

The parallel feed multiple effect evaporation is the industrial standard for seawater desalination using the multiple effect evaporation process. The parallel feed configuration has several attractive features including simple process layout, stable and wide operating range. The process model and performance has similar features to the forward feed configuration. The following sections include models and analysis for the thermal and mechanical vapor compression processes of the parallel and parallel/cross flow configurations.

As discussed in previous sections, the MEE-MVC system is thought to increase the system capacity. As will be shown later, use of this configuration has no effect on the specific power consumption. The market share of the MEE-MVC is less than 1%. On the other hand, the MEE-TVC has a higher share close to 5%. Both processes have attractive features that make them highly competitive against other well-established desalination processes that include the MSF and RO.

Limited number of field studies can be found on the MEE-TVC system, which include the following:

- Michels (1993) reported a number of outstanding features for the MEE process when combined with thermal vapor compression (MEE-TVC). These features include low corrosion and scaling, which is caused by low temperature operation (top brine temperature below 60°C). Other features include low energy consumption, short delivery time, easy operation and maintenance, proven reliability in the Gulf region. The cost of the plant erection, civil work, and the seawater intake is 35% cheaper than the MSF plants. Michels (1993) described three low capacity units of MEE with thermal vapor compression built in the remote western areas of the Emirate

of Abu Dhabi, UAE. The plants superseded the more classic multi stage flash (MSF) in the range of unit productions up to about $10x10^3$ ton/day.

- Temstet and Laborie (1996) outlined the main characteristic of a dual-purpose multi-effect desalination plant. The system is designed to switch automatically between two operating modes, which depends on the seasonal variations in power and water demand. The first mode combines the MEE system with a single-stage steam jet ejector, which compresses the vapor extracted from the last effect. The second mode of operation involves the use of low pressure heating steam. The plant operates over a low temperature ranges, includes 12 effects, and has a production capacity of 12000 m^3/day.

Other studies of the MEE-TVC system focus on modeling and performance evaluation. Examples for these studies include the following:

- Minnich et al. (1995) developed a simple model for the MEE-TVC system. The MEE system operates at low temperatures and in the parallel mode. The model is used to compare the performance and capital cost of the MEE-TVC versus the MSF and MEE systems. The capital cost for the three systems is based on the total heat transfer area. Several simplifying assumptions are used to develop the model and it includes:
  - Constant and equal temperature losses in all effects,
  - Constant and equal overall heat transfer coefficients in all effects,
  - Constant thermal load in all effects,
  - Negligible distillate flashing,
  - No feed preheaters,
  - Equal feed flow rates in all effects,
  - Negligible difference of latent heat and vapor enthalpy,
  - Constant specific heat and vapor enthalpy, and
  - Negligible pressure losses in the system components, demister and connecting tubes.

The model results show that operation of the MEE-TVC system at low top brine temperatures, 60 °C, gives higher heat transfer areas than the MSF system at performance ratios higher than 6. The capital cost the low temperature MEE-TVC system exceeds the MSF at performance ratios higher than 8. Merits of the MEE-TVC are only realized at higher top brine temperatures.

- Darwish and El-Dessouky (1995) developed a simple model for parallel feed MEE-TVC. The model includes balance equations for energy and mass in each effect and in the steam jet ejector. The ejector model is based on the graphical performance data for steam jet ejectors presented by Power (1994). The model assumes negligible pressure losses within the system components, constant and equal boiling point rise in all effects, and constant temperature drop per effect. In addition, the model did not include equations for the heat transfer areas and the distillate flashing boxes. The model is used to analyze a four-effect MEE-TVC system and results gave a performance ratio of 7.65 for a top brine temperature of 62 °C. The simplicity of the model imposes restrictions

on its use for system design or analysis. For example, a constant temperature drop per effect when used to calculations of the heat transfer area would result in varying area in the system effect. This result is the opposite of industrial practice, where constant heat transfer area is used in all effects to reduce construction and maintenance cost.

- El-Dessouky (1997) and El-Dessouky et al. (1998) developed extensive mathematical models for the single effect thermal vapor compression process (TVC) and the multiple effect systems (MEE). The model, results, and analysis for the single-effect TVC and the stand alone MEE form the basis for development of the more complex MEE-TVC model. Development of both models addressed the limitations found in previous literature studies. Discussion and details of the MEE system are presented in the previous chapter. As for the TVC model, it includes analysis of the evaporator/condenser and the steam jet ejector units. The model includes the energy and material balance equations for the evaporator/condenser, the ejector design equation, the heat transfer design equation for the evaporator/condenser, and correlations for the heat transfer coefficient, thermophysical properties, and thermodynamic losses. Predictions show that the performance ratio varies between 1 and 2 as the top brine temperature is increased from 60 to 100 °C. The performance ratio increases as the pressure of the motive steam is increased. This makes the motive steam capable of compressing larger amounts of the entrained vapor. As a result, the amount of motive steam is reduced causing the increase of the performance ratio. The system performance ratio is found to increase at lower compression ratios (pressure of compressed vapor/pressure of entrained vapor). At low compression ratios, the amount of motive steam required to compress the entrained vapor are smaller and as a result the system performance ratio increases. Lower heat transfer areas for the evaporator condenser are predicted at higher top brine temperatures, because of the increase in the overall heat transfer coefficient at higher temperatures. The specific flow rate of cooling water is found to decrease as the amount of entrained vapor to the steam ejector is increased. The behavior occurs at high top brine temperature, low motive steam pressures, and high compression ratios.
- El-Dessouky and Ettouney (1997) presented analysis of the MEE-TVC system. The developed MEE-TVC model is based on the two models developed by El-Dessouky (1997) for the single-effect TVC and the multiple effect MEE model developed by El-Dessouky et al. (1998). As a result, the MEE-TVC model is based on sound physical phenomena, which relates various processes occurring in the system. The model results show large increase in the system performance ratio over the stand alone MEE system, with increase varying from 20-50%. In addition, large reduction is obtained in the specific flow rate of cooling water.

5.1.1 Process Description

Figs. 1a and 1b show the MEE-P/TVC and MEE-PC/MVC processes. As is shown both systems include n effects and n-1 flashing boxes. Each effect includes a vapor space, demister, condenser/evaporator tubes, brine spray nozzles, and brine pool. In either system, the effects are numbered 1 to n from the left to right (the direction of the heat flow). Vapor flows from left to right, in the direction of falling pressure, while the feed seawater flows in a perpendicular direction. Compressed vapor is introduced into the tube side in the first effect; while, on the shell side feed seawater is sprayed on the tubes top rows. The brine spray forms a thin falling film on the succeeding rows within the evaporator. In the first effect, the brine falling film absorbs the latent heat of the compressed vapor. As a result, the brine temperature increases to saturation, where, evaporation commences and a smaller amount of vapor forms. This vapor is used to heat the second effect, where, it condenses on the tube side and releases its latent heat to the brine falling film. This process is repeated for all effects, until effect n.

In both systems, the condensed vapor in effects to 2 to n is introduced into the associated flashing box, where the temperature of the condensed vapor is reduced through flashing of a small amount of vapor. The flashed off vapor is routed into the tube side of the next effect together with the vapor formed by boiling or flashing within the previous effect.

In the MEE-P/TVC system, the vapor formed in the last effect is introduced into the down condenser. A controlled amount of intake seawater is routed into the tube side of the down condenser, where it condenses part of the vapor formed in the last effect. The steam jet ejector entrains the remaining part of the vapor, where it is compressed by the motive steam to the desired pressure and temperature. The warm intake seawater stream leaving the down condenser is divided into two parts; the first is the feed seawater stream, which is distributed among the evaporation effects, and the second is the cooling seawater stream, which is reject back to the sea. The cooling seawater stream removes the heat added to the system by the motive steam.

In the converging section of the steam jet ejector the kinetic energy of the motive steam increases drastically and its speed becomes supersonic near the contraction point. Consequently, its pressure drops to low values and allows for suction of the entrained vapor. Mixing of the motive steam and the entrained vapor takes place past the ejector contraction. In the diverging section, the mixture velocity is reduced, while, its pressure starts to increase. The compression process is controlled by the ejector geometry and the motive steam properties.

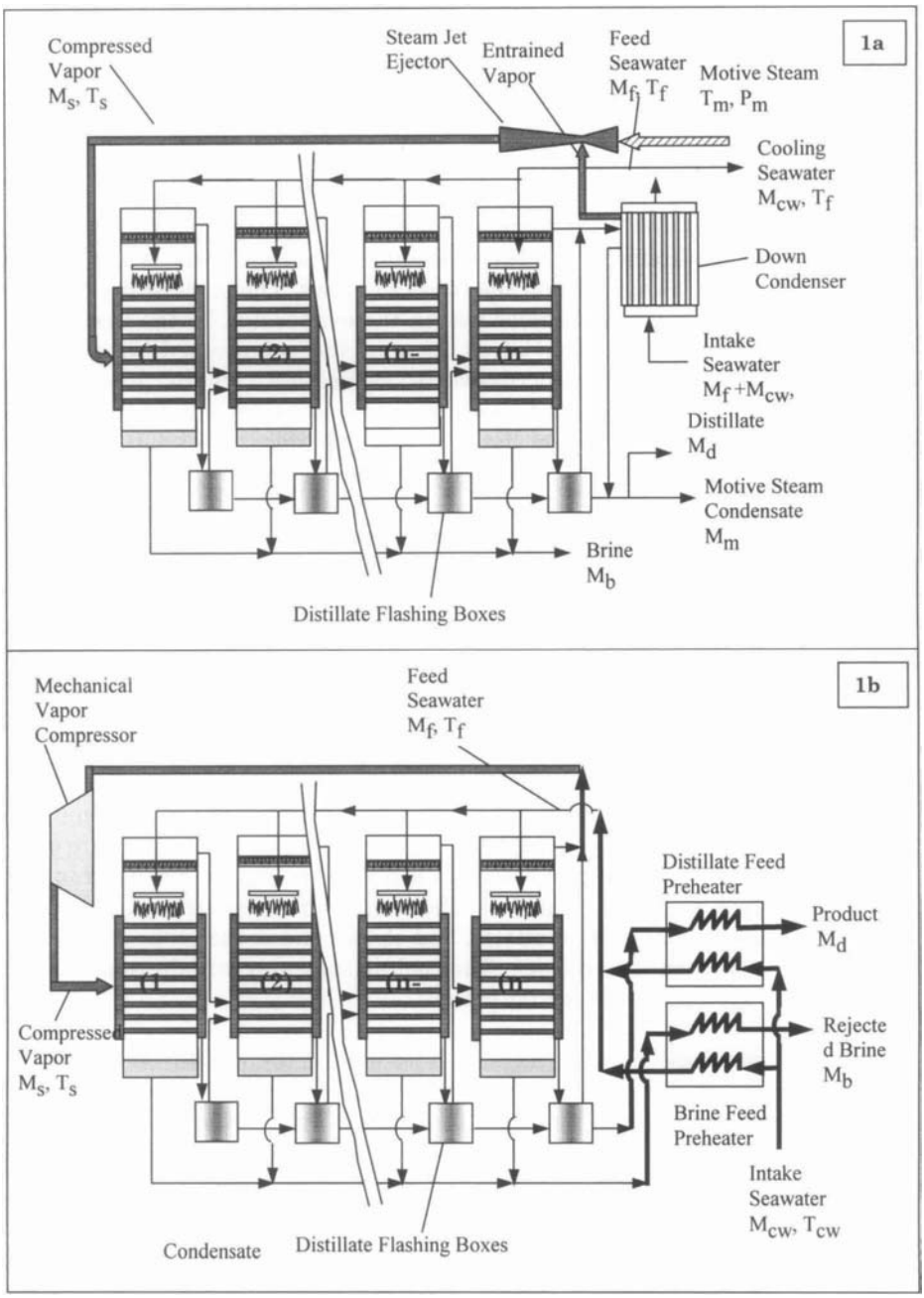

Fig. 1. Schematic of multiple effect evaporation with vapor compression(1a: parallel feed thermal vapor compression, MEE-P/TVC) and (1b: Parallel feed mechanical vapor compression, MEE-P/MVC).

The mechanical vapor compression system is distinguished by absence of the down condenser and use of the feed preheaters. Removal of the down condenser is a result of routing the entire vapor formed in the last effect to the mechanical vapor compressor, where the vapor is superheated to the desired temperature and pressure. At the other end, the feed preheaters recover part of the sensible heat found in the rejected brine and distillate product streams. This improves the system thermal efficiency and maintains production at the design levels, especially, during winter operation.

The main difference of the MEE-P and MEE-PC is that in the later system, the brine leaving effect (i) is introduced into the brine pool of effect (i+1). As a result of the positive temperature difference for the brine of effects (i) and (i+1), a small portion of the feed brine flashes off as it is introduced into effect (i+1). The flashed off vapors improves the system productivity and thermal efficiency. In effect (i+1), the flashed off vapors are added to the vapor formed by boiling within the same effect. As for the MEE-P process, the brine leaving each stage is directly rejected to the sea.

5.1.2 Process Modeling

Similarities among various systems considered in this analysis necessitate simultaneous development of the balance equations for various components within each system. Common assumptions among various models include steady state operation, constant heat transfer area in each effect, negligible heat losses to the surroundings, and salt free distillate product.

The following sections include discussion of the model equations for various components within the MEE-PC system. The model equations for the MEE-P system are not given, because of the similarity with the MEE-PC system. However, the discussion points to differences in balance equations of the MEE-P system. As for the correlations used to calculate the thermodynamic losses, pressure drops, and physical properties are given in the appendix. Fig. 2 shows a schematic for the system variables in the evaporator and the associated flash box in effect i. The figure includes flow rates, salinity, and temperatures of various streams as it enters and leaves the evaporator and the flashing box.

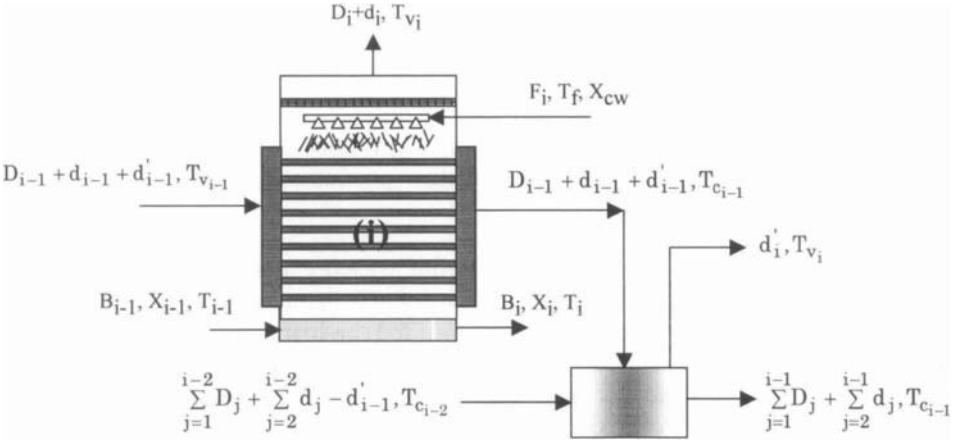

Fig. 2. Variables in evaporator and flash box of effect i.

Balance Equations for Each Effect

The mathematical model for each effect includes the material and energy balances as well as the heat transfer equation. The model includes the following equations:

- Total balance in effect i

$$F_i + B_{i-1} = D_i + B_i \tag{1}$$

- Salt balance in effect i

$$X_{F_i} F_i + X_{B_{i-1}} B_{i-1} = X_{B_i} B_i \tag{2}$$

In Eqs. 1 and 2, B, D, and F are the flow rates of brine, distillate, and feed, X is the salinity, and the subscripts B, F, and i designate the brine, feed, and the effect number.

- Rejected brine salinity

$$X_b = 0.9(457628.5–11304.11T_b+107.5781T_b^2–0.360747T_b^3) \tag{3}$$

This equation is used to calculate the reject brine salinity in each effect as a function of the brine temperature. This equation is obtained by curve fitting of the salinity/temperature relation for the solubility 90% of the solubility of $CaSO_4$. The upper limit on the rejected brine salinity is set at 70,000 ppm.

- Energy balance for effect i

$$D_{i-1}\,\lambda_{i-1} + d_{i-1}\,\lambda_{i-1} + d'_{i-1}\,\lambda'_{i-1} = F_i\,C_p(T_i - T_f) + D_i\lambda_i \quad (4)$$

In the above equation d is the amount of vapor formed by brine flashing in effect i-1, d' is the amount of vapor formed by flashing in the flashing boxes, λ is the latent, C_p is the specific heat at constant pressure, T_i is the brine boiling temperature, and T_f is the feed seawater temperature. In Eq. (4) the first term corresponds to the heat added to the effect by condensing the vapor generated in the previous effect. This only applies to effects 2 to n, since heating steam from an external source is used to drive the system and heat the first effect. In effect 3 to n, the second term in Eq. (4) defines the amount of heat associated with condensation of the vapor formed by brine flashing in the previous effect. The third term, which applies only to effects 3 to n, corresponds to the heat added to the effect by condensing the vapor generated in the distillate flashing box associated with the previous effect. The fourth term in Eq. 4 gives the amount of heat gained by the feed stream, where its temperature increased inside the effect from the seawater temperature to the brine boiling temperature. The last term gives the amount of heat consumed by the vapor generated inside the effect. In the above equation the specific heat at constant pressure depends on the brine salinity and temperature, while the latent heat depends on the vapor temperature. Correlations for the two properties are given in the appendix.

- Vapor temperature in effect i

$$T_{vi} = T_i - BPE_i \quad (5)$$

where BPE is the boiling point elevation and T_v is the vapor temperature.

- The vapor condensation temperature

$$T_{ci} = T_i - BPE_i - \Delta T_p - \Delta T_t - \Delta T_c \quad (6)$$

In Eq. 5, the condensation temperature, T_{ci}, is lower than the brine boiling temperature, T_i, by the boiling point elevation and the losses caused by pressure depression in the demister (ΔT_p), friction in the transmission line (ΔT_t), and during condensation (ΔT_c).

- Amount of vapor formed by brine flashing inside the effect

$$d_i = B_{i-1}\,Cp\,\frac{T_{i-1} - T'_i}{\lambda_i} \quad (7)$$

with

$$T'_i = T_i + NEA_i \quad (8)$$

In Eq. 7, T_i' is the temperature to which the brine cools down as it enters the effect. Also, the latent heat λ_i is calculated at the effect vapor temperature, T_{v_i}. The term $(NEA)_i$ is the non-equilibrium allowance and is calculated from the correlation developed by Miyatake (1973):

$$(NEA)_i = \frac{33.0\,(T_{i-1} - T_i)^{0.55}}{T_{v_i}}$$

– Amount of vapor flashed off in the distillate flashing boxes

$$d_i' = D_{i-1} C_p \frac{(T_{c_{i-1}} - T_i'')}{\lambda_i'} \tag{9}$$

with

$$T_i'' = T_{v_i} + (NEA)_i$$

where $(NEA)_i$ is the non-equilibrium allowance and is equal to $(NEA)_i = 0.33\frac{(T_{c_{i-1}} - T_{v_i})}{T_{v_i}}$, T_i'' is the temperature to which the condensing vapor cools down to as it enters the flashing box.

– Heat transfer area in effect i

$$D_{i-1}\,\lambda_{i-1} + d_{i-1}\,\lambda_{i-1} + d_{i-1}'\,\lambda_{i-1}' = F_i\,C_p(T_i - T_f) + D_i\lambda_i$$
$$= A_{1i}\,U_{1i}\,(LMTD)_i + A_{2i}\,U_{2i}\,(T_{c_i} - T_i) \tag{10}$$

$$\alpha(D_{i-1}\,\lambda_{i-1} + d_{i-1}\,\lambda_{i-1} + d_{i-1}'\,\lambda_{i-1}') = D_i\lambda_i = A_{2i}\,U_{2i}\,(T_{c_i} - T_i) \tag{11}$$

$$(LMTD)_i = (T_i - T_f)/\ln((T_{c_i} - T_f)/(T_{c_i} - T_i)) \tag{12}$$

where A_{1i} is the heat transfer area for sensible heating of the brine from the feed to the boiling temperature in each effect and A_{2i} is the heat transfer area for evaporation, U_{1i} and U_{2i} are the corresponding overall heat transfer coefficient, LMTD is the logarithmic heat transfer coefficient, and α is the fraction of input heat consumed by vapor formation.

Balance Equations for the Down Condenser

The down condenser balance equations include the energy balance and heat transfer rating equation.

- Energy balance of the down condenser

$$(d_n + d'_n + D_n)\lambda_n = (M_{cw} + M_f)\, Cp\, (T_f - T_{cw}) \tag{13}$$

- Rating of the down condenser

$$(d_n + d'_n + D_n)\lambda_n = U_c\, A_c\, (LMTD)_c \tag{14}$$

$$(LMTD)_c = (T_f - T_{cw})/\ln((T_{v_n} - T_{cw})/(T_{c_n} - T_f)) \tag{15}$$

where A_c, U_c, and $(LMTD)_c$ are the heat transfer area, overall heat transfer coefficient, and logarithmic mean temperature difference.

In presence of the steam jet ejector, the thermal load of the down condenser is lower since the part of the vapor formed in the last effect and the associated flashing box is entrained in the steam jet ejector. Therefore, the vapor formed in the last effect is defined by

$$M_{ev} + M_u = (d_n + d'_n + D_n) \tag{16}$$

where M_{ev} and M_u are the flow rates of the entrained and un-entrained vapor, respectively. In the following section, which includes the steam jet ejector model, the flow rate of the entrained vapor is obtained from the ejector entrainment ratio.

Model of the Steam Jet Ejector

The steam jet ejector is modeled by the semi-empirical model developed by El-Dessouky (1997). The model makes use of the field data collected over 35 years by Power (1994) for vapor entrainment and compression ratios of steam jet ejectors. The compression ratio, Cr, is the pressure ratio of the compressed and entrained vapors. The entrainment ratio is flow rate ratio of the motive steam and the entrained vapor. The entrainment ratio, Ra, is calculated from the following relation

$$Ra = 0.296 \frac{(P_s)^{1.19}}{(P_{ev})^{1.04}} \left(\frac{P_m}{P_{ev}}\right)^{0.015} \left(\frac{PCF}{TCF}\right) \tag{17}$$

where, P_m, P_s and P_{ev} are the pressures of the motive steam, compressed vapor, and entrained vapor respectively, PCF is the motive steam pressure correction factor and TCF is the entrained vapor temperature correction factor. The following two equations are used to calculate PCF and TCF

$$PCF = 3x10^{-7} (P_m)^2 - 0.0009 (P_m) + 1.6101 \quad (18)$$

$$TCF = 2x10^{-8} (T_{ev})^2 - 0.0006 (T_{ev}) + 1.0047 \quad (19)$$

where P_m is in kPa and T_{ev} is in °C. The previous equations are valid only for ejectors operating with steam as the motive fluid and the entrained gas is water vapor. These equations are valid in the following ranges: $Ra \leq 4$, $500 \geq T_{ev} > 10$ °C, $3500 \geq P_m \geq 100$ kPa, and $6 \geq Cr = \frac{P_s}{P_{ev}} \geq 1.81$.

The steam jet ejector must be designed and operated at critical conditions to allow normal and stable operation. This condition is associated with absence of violent fluctuations in the suction pressure. If the ejector is designed to operate with a full stable range, it will have a constant mass flow rate of the entrained vapor for different discharge pressures when the upstream conditions remain constant. The ejector is critical when the compression ratio is greater than or equal to the critical pressure ratio of the suction vapor. For water vapor this ratio is 1.81. That is, the suction pressure must be less than 0.55 times the discharge pressure to obtain critical or stable conditions in the steam jet ejector. The above limit on the compression ratio necessitates the use of two steam jet ejectors in series, Fig. 3, for a wide compression range. For example, in a single jet ejector that compresses a vapor to 80 °C and entrains vapor at 38 °C, the compression ratio in 7.14. This compression value requires the use of two ejectors in series, where the compression range is divided over the two ejectors. The corresponding balance equations for two ejectors in series include the following:

$$M_s = M_{s1} + M_{m2} \quad (20)$$

$$M_{s1} = M_{ev} + M_{m1} \quad (21)$$

$$Ra_1 = M_{m1}/M_{ev} \quad (22)$$

$$Ra_2 = M_{m2}/M_{s1} \quad (23)$$

$$Cr_1 = P_{s1}/P_{ev} \quad (24)$$

$$Cr_2 = P_s/P_{s1} \quad (25)$$

where M is the mass flow rate and the subscripts ev, m, s, 1, and 2 define the entrained vapor, the motive steam, the compressed, first and second ejector.

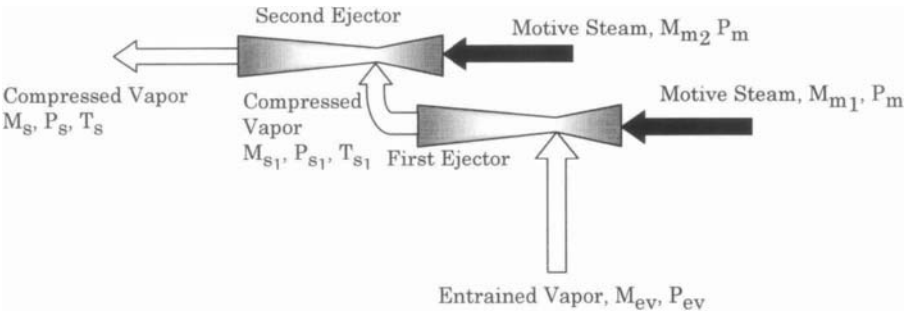

Fig. 3. Schematic of the two ejectors in series.

Model of the Mechanical Vapor Compressor

The specific power consumption of the compressor

$$Q_c = W \rho_d/3600 \tag{26}$$

where ρ_d is the density of distillate product, W is the actual specific work of the compressor, which is given by

$$W = H_s - H_v \tag{27}$$

The enthalpies H_s and H_v are calculated at the compressed vapor temperature, T_s, and the formed vapor temperature in the last effect, T_{vn}, which is lower than $\overline{T}_{vn}$ by the temperature depression caused by pressure drop in the demister. The compressor polytropic specific work is given by

$$\frac{W_m}{W_n} = \eta \left[\frac{(P_s/P_v)^{(\gamma-1/\gamma\eta)} - 1}{(P_s/P_v)^{(\gamma-1/\gamma)} - 1} \right] \tag{28}$$

In Eq. 28 the adiabatic compressibility factor is defined as

$$\gamma = \frac{1}{1 - (1+X)^2 (ZR/Cp_v)/Y} \tag{29}$$

where $X = 0.1846\ (8.36)^{(1/Z)} - 1.539$ and $Y = 0.074\ (6.65)^{(1/Z)} + 0.509$, ASHRAE (1997). In Eq. 29, the compressibility factor Z is set equal 1. The compressor

adiabatic work, W_n, given in Eq. 28 is defined as the enthalpy difference of the in terms of the

$$W_n = H_n - H_v \tag{30}$$

In Eq. 30 H_n and H_v are calculated at T_n and T_{v_n}, respectively, where T_n is calculated from the relation

$$T_n = T_{v_n} (P_v/P_n)^{(\gamma-1)/\gamma} \tag{31}$$

The enthalpy and temperature of the superheated (or compressed vapor) are obtained from the following relations

$$\eta = \frac{W_m}{H_s - H_v} \tag{32}$$

$$H_s = H_d + Cp_v (T_s - T_d) \tag{33}$$

where H_d and T_d are the saturation enthalpy and temperature of the compressed vapor, and H_s and T_s are the superheat enthalpy and temperature of the compressed vapor.

Preheaters Models

Two preheaters are used to increase the intake seawater temperature in the MEE-P/MVC system. This temperature increase is an essential part in energy recovery within the system and it has a strong effect on the plant performance or the specific power consumption. Heating of the feed seawater is performed against the hot product and brine streams leaving the last effect. This process takes place in two plate type heat exchange units, where the intake seawater is divided into two portions, αM_f and $(1-\alpha)M_f$. In the first preheater, heat is exchanged between αM_f and the product water, and in the second preheater, heat is exchanged between $(1-\alpha)M_f$ and the rejected brine. The sum of the thermal load for the two heat exchangers is given in terms of the intake seawater temperature increase. This is

$$Q_h = M_f C_p (T_f - T_{cw}) \tag{34}$$

where Q_h is thermal load of the two preheaters, Cp is the specific heat at constant for the seawater, T_f is feed seawater temperature, and T_{cw} is the intake

seawater temperature. Equation (34) can be also written in terms of the heat load of the product water and the rejected brine, which gives

$$Q_h = M_d\, C_p\, (T_{c_n} - T_o) + M_b\, C_p\, (T_n - T_o) \tag{35}$$

Where T_{c_n} and T_n are the temperatures of the product water and brine leaving the last effect and T_o is the temperature of both streams after leaving the preheaters. Equations 34 and 35 are equated and the result is used to determine the outlet temperature of the heating streams, T_o,

$$M_f\, C_p\, (T_f - T_{cw}) = M_d\, C_p\, (T_{c_n} - T_o) + M_b\, C_p\, (T_{c_n} - T_o) \tag{36}$$

The driving force for heat transfer in the preheaters is taken as the logarithmic mean of the temperature difference at both ends of the preheater. These equations are given by

$$A_d = \frac{M_d C_p (T_{c_n} - T_o)}{U_d (LMTD)_d} = \frac{\alpha M_f C_p (T_f - T_{cw})}{U_d (LMTD)_d} \tag{37}$$

$$\begin{aligned} A_b &= \frac{M_b C_p (T_n - T_o)}{U_b (LMTD)_b} \\ &= \frac{M_d (X_f / (X_b - X_f)) C_p (T_n - T_o)}{U_b (LMTD)_b} \\ &= \frac{(1-\alpha) M_f C_p (T_f - T_{cw})}{U_b (LMTD)_b} \end{aligned} \tag{38}$$

The $(LMTD)_d$ is defined as:

$$(LMTD)_d = \frac{(T_{c_n} - T_f) - (T_o - T_{cw})}{\ln \dfrac{T_{c_n} - T_f}{T_o - T_{cw}}} \tag{39}$$

The $(LMTD)_b$ is defined as:

$$(LMTD)_b = \frac{(T_n - T_f) - (T_o - T_{cw})}{\ln \dfrac{T_n - T_f}{T_o - T_{cw}}} \tag{40}$$

Solution Algorithm

The mathematical models for either system are interlinked and highly nonlinear. Therefore, iterative solution is necessary to calculate the system characteristics. The solution algorithm starts with definition of the following parameters:

- The number of effects varies over a range of 4-12.
- The heating steam temperature varies over a range of 60-100 °C.
- The seawater temperature (T_{cw}) is 25°C.
- The seawater salinity has values of 34,000 ppm or 42,000 ppm.
- The temperature of rejected cooling water or feed seawater (T_f) is less than condensing vapor temperature (T_{c_n}) by 5 °C.
- The boiling temperature in the last effect (T_n) is 40°C.
- The specific heat at constant pressure of the vapor, C_{p_v}, is 1.884 kJ/kg °C.
- The polytropic efficiency of the compressor, η, is 0.76 [24].

The solution algorithm for the thermal vapor compression system is shown in Fig. 4. As is shown, the model equations are solved simultaneously by Newton's method to calculate the following:

- The flow rates, salinity, and temperatures of the feed, brine, and distillate in each effect.
- The heat transfer area for evaporation and sensible heating in each effect.
- The fraction of heat consumed by evaporation in each effect.
- The above results are used to calculate the following:
- The heat transfer area in the condenser.
- The flow rate of cooling seawater.
- The entrainment ratio in the steam jet ejector.
- The amount of motive steam.

Figure 5 shows the solution algorithm for the mechanical vapor compression system. In this system, the amount of compressed vapor is known and is equal to the amount of vapor formed by boiling in the last effect as well as the amount of vapor formed by brine and distillate flashing. The energy and material balance model as well as the compressor model are solved simultaneously and iteratively by Newton's method. Simultaneous solution of the two models gives the following system variables:

- Temperature, salinity, and flow rate profiles of feed, distillate, and brine streams.
- The specific power consumption of the mechanical vapor compressor.
- The temperature of the compressed vapor.
- The heat transfer areas for vapor formation and brine heating in each effect.
- The heat transfer area of the feed preheaters.

The Newton's iterative procedure has an iteration error of $1x10^{-4}$. To facilitate the conversion procedure, each equation is scaled by the largest term found in the equation. Therefore, all equations are in the order of one. For example, the salt balance equation is rearranged into the following form

$$f(X_{cw}, F_i, X_{b_i}, B_i) = 1 - (X_{cw} F_i)/(X_{b_i} B_i)$$

Convergence of Newton's method is dependent on the initial guess, therefore, linear profiles are used for the flow rates, brine temperature, heat transfer areas, and the ratio α. The guess for the steam flow rate is based on the approximate relation of the number of effects and the performance ratio.

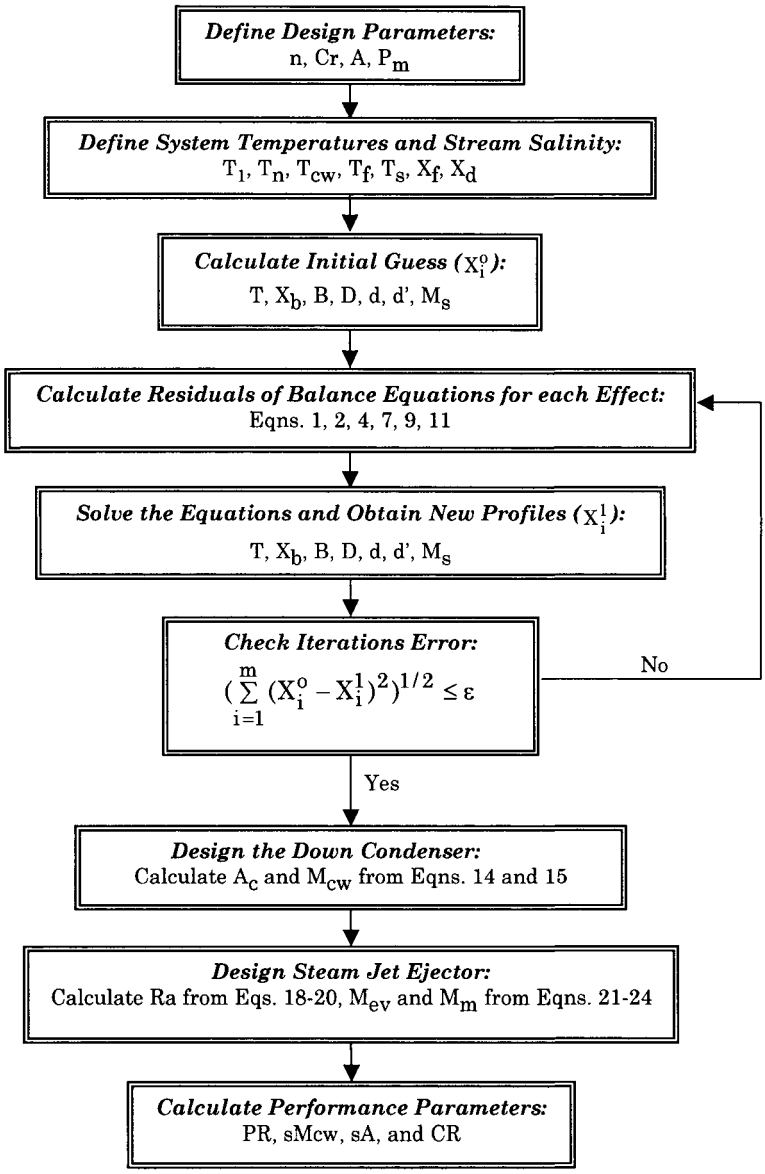

Fig. 4. Solution algorithm of the thermal vapor compression system.

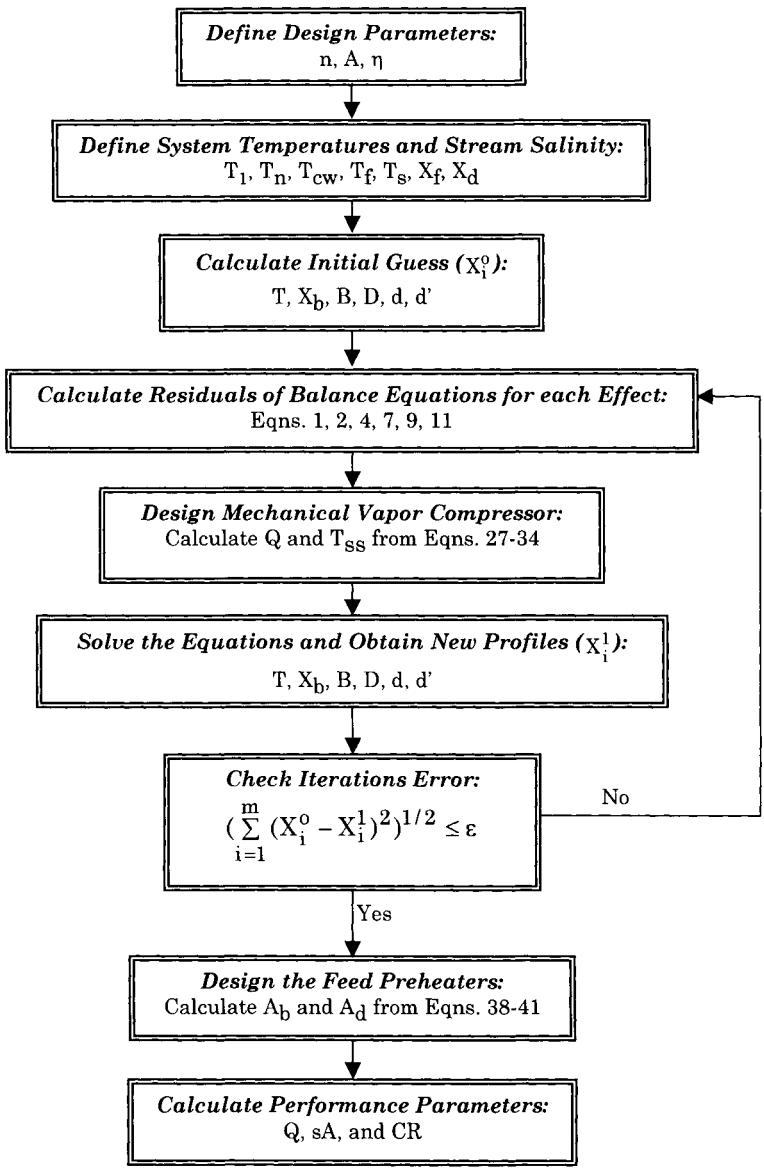

Fig. 5. Solution algorithm of the mechanical vapor compression system.

5.1.3 System Performance

Characteristics of the thermal vapor compression systems are obtained as a function of the heating steam temperature. Figure 6 shows variations in the thermal performance ratio for the MEE-P/TVC and MEE-PC/TVC for 8 effects, motive steam pressure of 1500 kPa, and a compression ratio of 4. As is shown, the performance ratio decreases with the increase in the top brine temperature. Also, at low top brine temperatures the thermal performance ratio for vapor compression units is close to 75-100% higher than the stand-alone systems. For example at a top brine temperature of 60 °C, the thermal performance ratio for the vapor compression units is 12.2 and is equal to 7.3 for the stand-alone units.

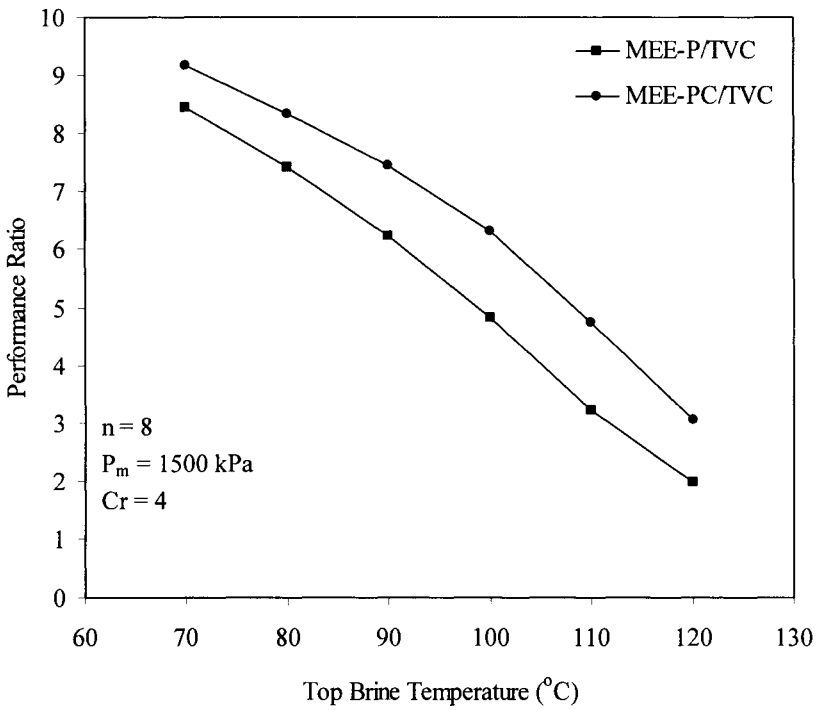

Fig. 6. Variation in the thermal performance ratio as a function of the top brine temperature

The reduction in the system thermal performance ratio at higher steam temperature is caused by the following factors:

- The reduction in compressed vapor latent heat, i.e., at 60 °C the latent heat is 2470 kJ/kg and at 110 °C it is equal to 2105 kJ/kg.

- The increase in the amount of feed sensible heating, since the feed temperature is kept constant at 35 °C.
- The increase in the amount of motive steam required for vapor compression at higher temperatures, since the entrained vapor is kept constant at a temperature below 40 °C.

Variations in the specific heat transfer area for both MEE-P/TVC and MEE-PC/TVC are shown in Fig. 7. As is shown the specific heat transfer area decreases rapidly as the heating steam temperature increases. The following effects cause this behavior:

- The increase in the overall heat transfer coefficient as a result of higher values for the physical properties of the brine and condensing vapor, which enhances the rate of heat transfer in either stream.
- The increase in the temperature driving force per effect, where at higher top brine temperatures and for the same number of effects causes the increase in the temperature drop per stage.

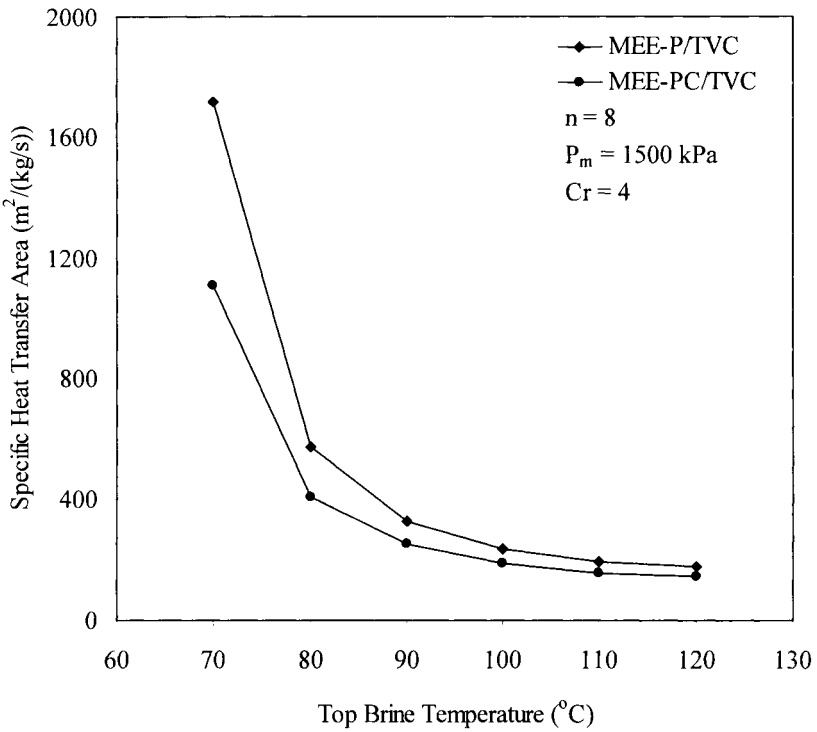

Fig. 7. Variation in the specific heat transfer area as a function of the top brine temperature

As is shown in Fig. 8, the conversion ratio for the MEE-PC/TVC is independent of the top brine temperature. On the other hand, the conversion ratio for the MEE-P/TVC system decreases with the increase of the top brine temperature. For the MEE-PC/TVC system the feed stream for all effects has a constant salinity of 42,000 ppm, and the salinity of the final brine stream is 70,000 ppm. Therefore, the balance equations for the system give a conversion ratio independent of the top brine temperature. As a result, the amount of feed seawater for the MEE-PC/TVC remains constant as the top brine temperature increases. As for the MEE-P/TVC system, the conversion ratio decreases with the increase in the heating stream temperature (Fig. 8). This is because of the reduction in the brine salinity at higher temperatures. Therefore, at higher temperatures the amount of feed seawater must be increased to account for the limits imposed on the brine salinity. This increase results in reduction in the amount of cooling seawater.

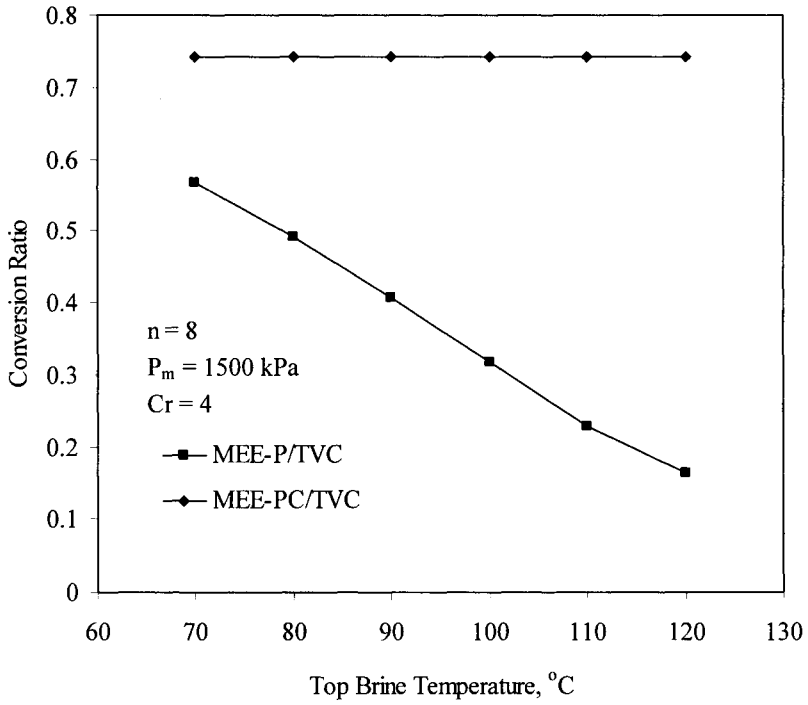

Fig. 8. Variations in the conversion ratio as a function of the top brine temperature.

Variations in the specific flow rate of cooling water for both systems are shown Fig. 9. As is shown, for MEE-PC/TVC system the specific flow rate of

cooling water decreases with the increase in the top brine temperature. This is because of the increase in the specific thermal load, or the decrease in the thermal performance ratio, and the constant conversion ratio, or a constant feed flow rate. Both effects require the increase in the specific flow rate of cooling water. The decrease in the specific flow rate for the cooling water in the MEE-P/TVC system at higher top brine temperatures is also caused by the decrease in the system conversion ratio or the increase in the amount of feed seawater.

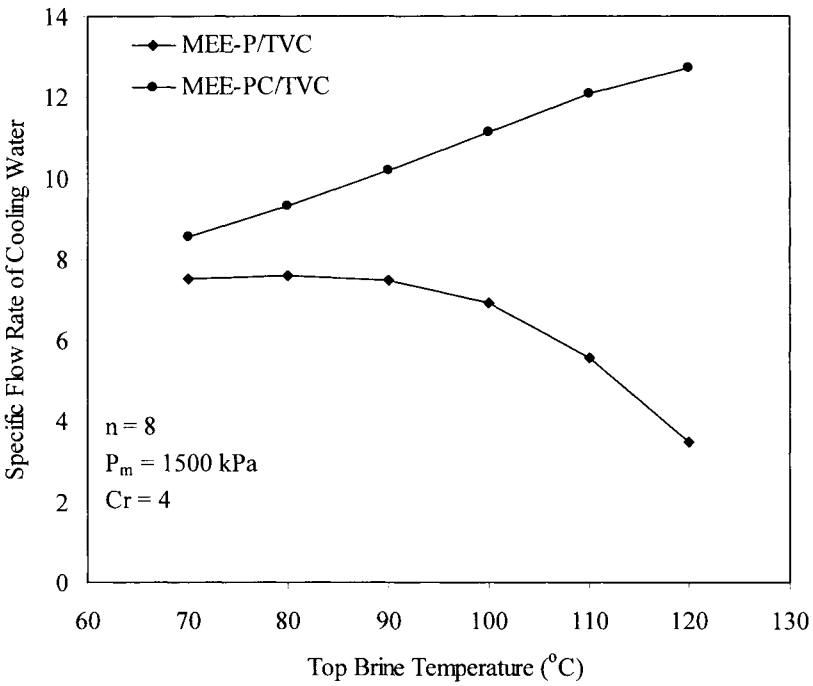

Fig. 9. Variation in the specific flow rate of cooling as a function of the top brine temperature

Analysis of the mechanical vapor compression systems shows high sensitivity to the range of operating parameters, especially, the temperature difference of the brine in the first and last effect and the temperature of the feed seawater. Calculations are performed for the following conditions:

- Top brine temperatures of 50, 60, 70, and 80 °C.
- Condensation temperatures of the compressed vapor are higher than the top brine temperature by 1, 2, 3, and 4 °C.

- Brine temperature in the last effect lower than the top brine temperature by 9 °C.
- Feed temperature lower than the brine temperature in the last effect by 2 °C.

The Results for four effects MEE-P/MVC system are shown in Figs. 10 and 11 for the specific heat transfer area and the specific power consumption, respectively. As is shown in Fig. 10, the specific heat transfer area decreases with the increase in the top brine temperature and the difference of the condensing vapor and top brine temperatures. On the other hand, the specific power consumption decreases with the increase in the top brine temperature and the decrease in the difference of the condensing vapor and the top brine temperatures, Fig. 11. The specific power consumption for the above set of parameters varies between low values close to 8 kWh/m^3 and higher values close to 12 kWh/m^3. Selection of the best design and operating conditions necessitates optimization among the specific heat transfer area and the specific power consumption.

In should be noted that the specific power consumption for the MEE-P/MVC and MEE-PC/VC have similar values at the same set of operating conditions (Fig. 11). This is consistent with the model of the compressor, since it depends on the amount of generated vapor in the last effect and flashing box, the compression range, and the temperatures of the intake and compressed vapor streams. For both systems the temperatures of the brine in the first effect, the intake vapor, and the compressed vapor are identical. However, in the MEE-PC/MVC system the amount of vapor generated in the last effect is slightly higher because of brine flashing.

As for the specific heat transfer area, values for the MEE-PC system are lower than the MEE-P system. This is because of direct rejection of the brine from each effect in the MEE-P system. On the other hand, the brine stream leaving each effect in the MEE-PC system is allowed to release part of its heat through flashing in subsequent effects.

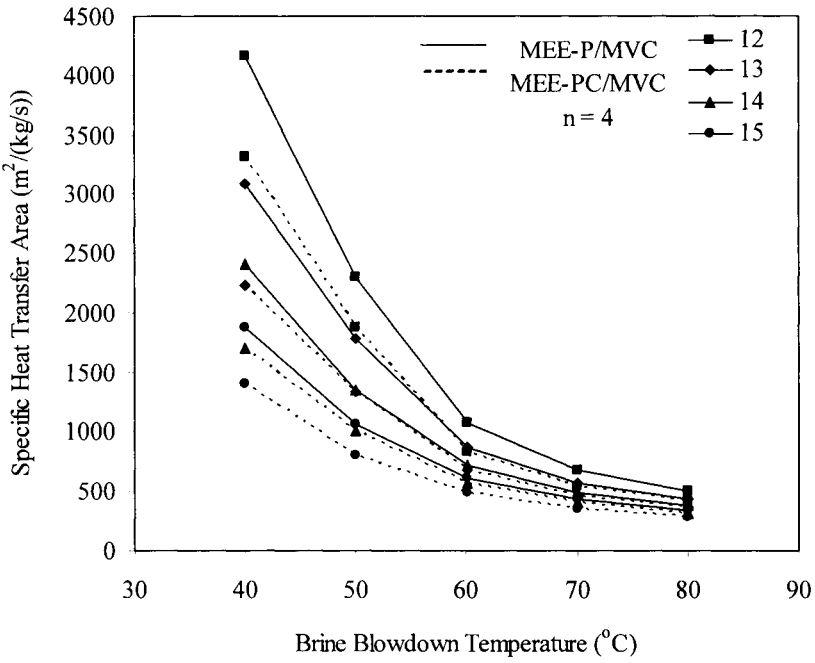

Fig. 10. Variation in the specific heat transfer area as a function of the brine blowdown temperature and the difference between condensing vapor and brine blowdown temperatures

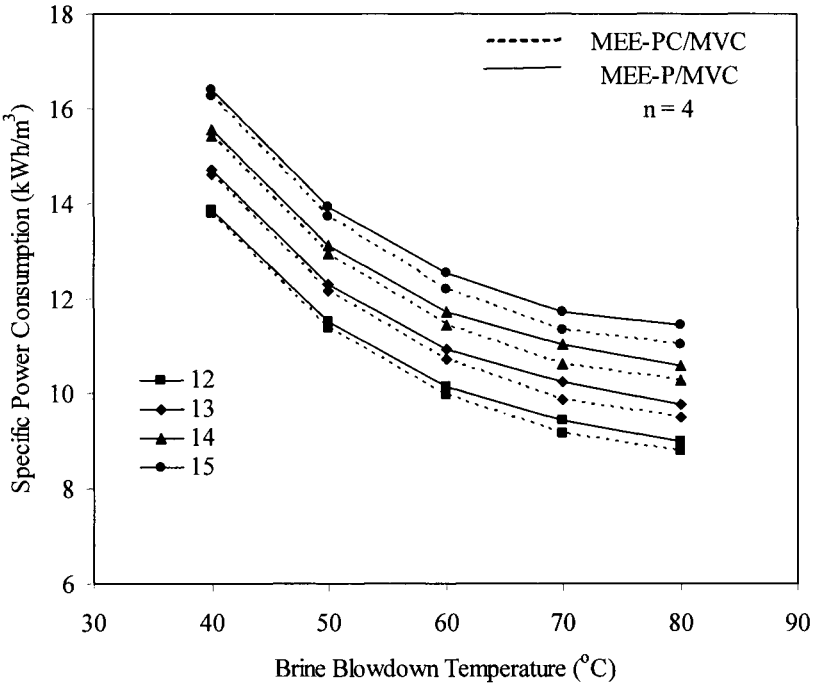

Fig. 11. Variation in the specific power consumption as a function of the brine blowdown temperature and the difference between condensing vapor and brine blowdown temperatures

5.1.4 Comparison with Industrial Data

Table 1 includes comparison of model predictions against two industrial MEE-PC/MVC systems. Literature review indicates that most of the existing MVC units are of the single effect type. It should be stressed that industrial use of the 3 and 4 effects systems is to increase the total system capacity rather than to decrease the specific power. Both systems operate in the MEE-PC mode, where the brine stream cascades across the effects. The results in Table 2 show good agreement between the predicted and actual specific power consumption. The relative error in the specific power consumption is below 9%. Comparison of the specific heat transfer area was not possible because no field data was available.

The data shown in Table 2 are obtained for multiple effect thermal vapor compression systems with 4, 6, and 12 effects. To obtain the model predictions, the system layout had to be arranged similar to the industrial configuration. Also, the temperatures of the heating steam, the last stage, the intake seawater,

and feed seawater are all defined. Other system definitions include the salinity of the intake seawater and rejected brine. The model is used to calculate the specific heat transfer area, the specific flow rate of cooling water, and the performance ratio. The comparison includes only the performance ratio and the specific flow rate of cooling water. No comparison was made for the specific heat transfer area, because, the field data was not available. As is shown, the model predictions compares well with the industrial data. The relative percentage error of model predictions to the industrial data is limited to values below 15%.

Table 1
Comparison of model predictions against field data for MEE-MVC systems.

Reference	Lucas and Tabourier (1985)	Model	Ophir and Gendel (1999)	Model
N	4	4	3	3
M_d (m^3/d)	1500	1500	3000	3000
T_s (°C)	62.5	62.5	70	70
T_n (°C)	50.7	50.7		
T_{cw} (°C)	5	5		
T_f (°C)	49	49		
X_{cw} (ppm)	36000	36000	36000	36000
X_{bn} (ppm)	64800	64800		
CR	0.446	0.446		
sA_c ($m^2/(kg/s)$)	–	2234		
Q (kWh/m^3)	11	10.7	6.9	6.3

Table 2
Comparison of model predictions against field data for MEE-TVC systems.

Process	Temstet et al. (1996)	Model	Weinberg and Ophir (1997)	Model	Michles (1993)	Model	Elovic and Willocks (1999)	Model
n	12	12	6	6	4	4	12	12
M_d (m^3/d)	$1.2x10^4$	$1.2x10^4$	$2.1x10^4$	$2.1x10^4$	$4.5x10^3$	$4.5x10^3$	$5.9x10^3$	$5.9x10^3$
T_s (°C)	70	70	62.9	62.9	62.7	62.7	71	71
T_n (°C)	38.5	38.5	36.3	36.3	48.4	48.4	40+	40
T_{cw} (°C)	29.5	29.5	26	26	33	33	30+	30
T_f (°C)	34.5	34.5	32	32	44	44	35+	35
X_{cw} (ppm)	36000	36000	42000	42000	47000	47000	36000+	36000
X_{bn} (ppm)	51730	51730	52900	52900	71500	71500	52000+	52000
CR	0.33	0.33	0.33	0.33	0.33	0.33	0.31+	0.31
sM_{cw}	6.212	6.8	11.9	12.4	3.79	4.31	–	7.2
sA_c ($m^2/(kg/s)$)	–	1385	–	734	–	523	–	1283
PR	13.4	14.1	5.7	6.2	8.6	9.3	11.5	11.9

+ Values assumed

5.1.5 Summary

System analysis is presented for two configuration of the parallel feed multiple effect evaporation. Each system is analyzed for the thermal and mechanical vapor compression modes. In the light of system analysis, the following conclusions are made:

- The thermal performance ratio for MEE-P/TVC and MEE-PC/TVC systems, especially at lower top brine temperatures, are more than 50-100% higher than the stand alone mode.
- The specific heat transfer area for all configurations, including thermal and mechanical vapor compression, decreases drastically at higher top brine temperatures because of the increase in the driving force for heat transfer.
- The specific power consumption for the mechanical vapor compression system have similar values for both systems since it depends on the temperature difference of the intake and compressed vapors as well as the top brine temperature, all of which were similar for both systems.
- The specific heat transfer area for the MEE-PC/MVC is lower than the MEE-P/MVC system. This is because of the increase in the total amount of product flow rate, which is caused by brine flashing within each effect.

References

ASHRAE Handbook – Fundamentals, ASHRAE, Atlanta, GA, USA, 1997.

Darwish M.A., and El-Dessouky, H., The heat recovery thermal vapour-compression desalting system: A Comparison with other thermal desalination Processes, Applied Thermal Engineering, 18(1996)523-537.

El-Dessouky, H.T., Modelling and Simulation of Thermal Vapor Compression Desalination Process, Proceedings of International Atomic Energy Agency, Symposium on Desalination of Seawater with Nuclear Energy, Taujon, Korea, 26-30 May (1997).

El-Dessouky, H.T., and Ettouney, H.M., Hybrid multiple effect evaporation/heat pump water desalination systems, 1st IDA Int. Desalination Conference in Egypt, Cairo, Egypt, September, 1997.

El-Dessouky, H., Alatiqi, I., Bingulac, S., and Ettouney, H., Steady-state analysis of the multiple effect evaporation desalination process, Chem. Eng. Technol., 21(1998)15-29.

Elovic, P., and Willocks, G., Case study of operating experience of 9 low-temperature MED plants in the US Virgin Islands, Proceedings of the IDA

World Conference on Desalination and Water Science, San Diego, USA, 1999, Vol. IV, pp. 143-152.

Lucas, M., and Tabourier, B., The Mechanical Vapour Compression Process Applied to Seawater Desalination: A 1500 ton/day Unit Installed in the Nuclear Power Plant of Flamanville, France, Desalination, **52**(1985)123-133.

Michles, T., Recent achievements of low temperature multiple effect desalination in the western areas of Abu Dhabi, UAE, Desalination, **93**(1993)111-118.

Minnich, K., Tonner, J., and Neu, D., A comparison of heat transfer requirement and evaporator cost for MED-TC and MSF, Proceedings of the IDA World Congress on Desalination and Water Science, Abu Dhabi, UAE, 1995, Vol. III, 233-257.

Miyatake, O., Murakami, K., Kawata, Y., and Fujii, Fundamental Experiments with Flash Evaporation, Heat Transfer Jpn. Res., **2**(1973)89-100.

Power, B.R., Steam Jet Ejectors for Process Industries, McGraw-Hill, New York, 1994.

Temstet, C., Canton, G., Laborie, J., and Durante, A., A large high-performance MED plant in Sicily, Desalination, **105**(1996) 109-114.

Weinberg, J., and Ophir, A., Ashdod experience and other dual purpose desalination plants based on multi effect desalination with aluminum tubes, Symposium of Desalination of Seawater with Nuclear Energy, Taejon, Republic of Korea, May, 1997.

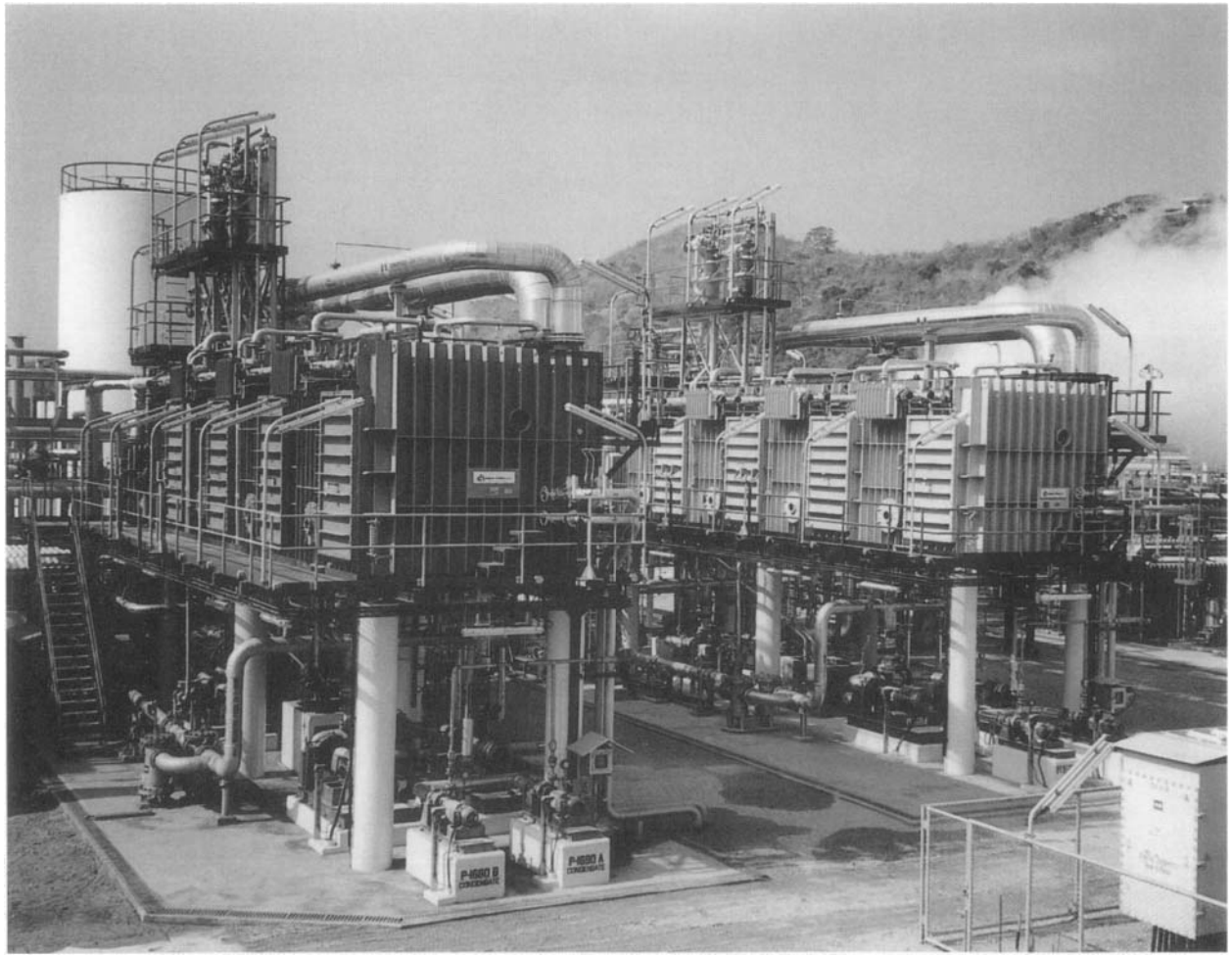
P-4680 B
CONDENSATE
P-4680 A
CONDENSATE

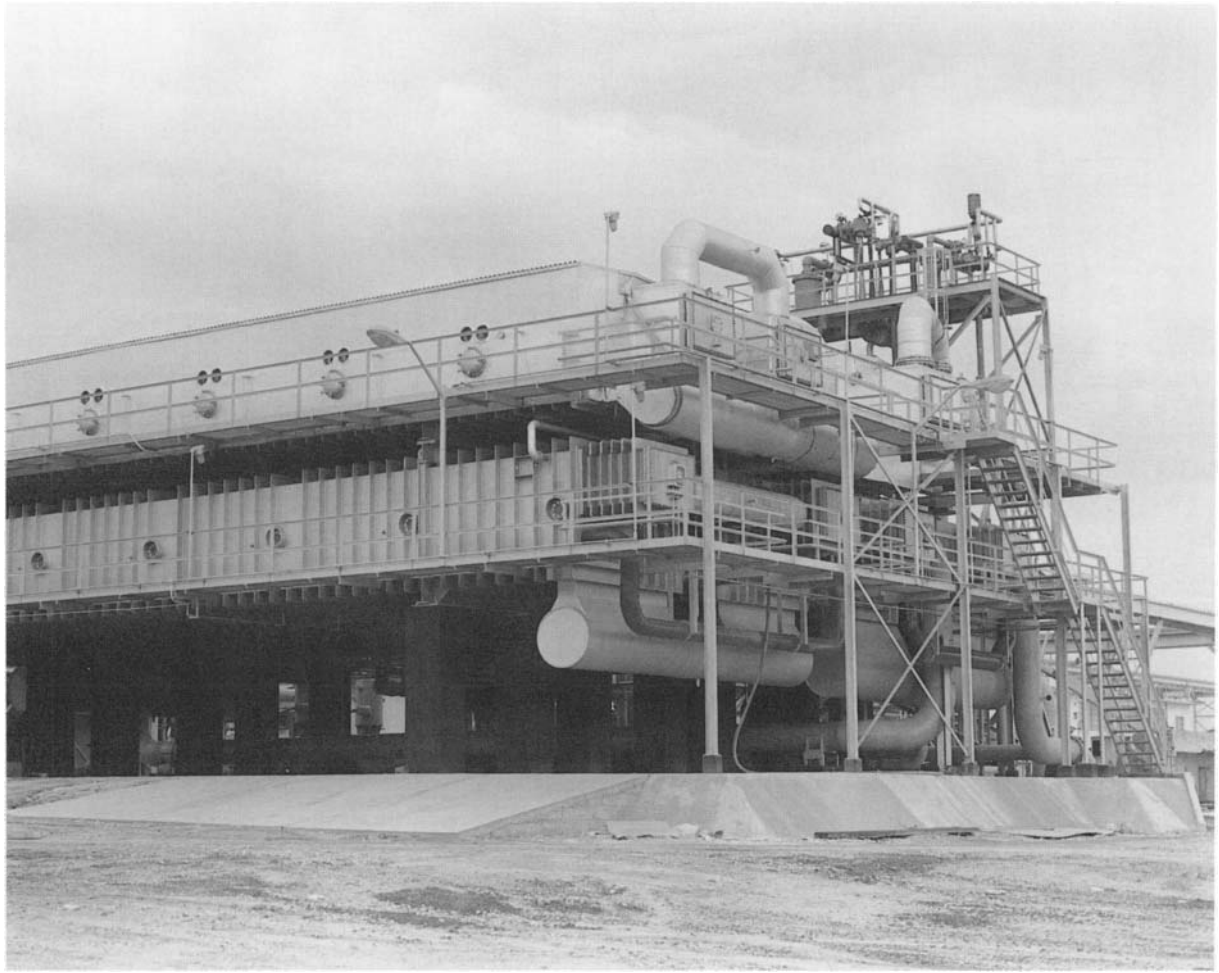

5.2 *Forward Feed Multiple Effect Evaporation Thermal Vapor Compression*

The forward feed thermal vapor compression system is illustrated in Fig. 12. Process elements are similar to the forward feed system given in chapter 4. Also, combining the system with thermal vapor compression has identical features to the parallel feed system given in the previous section.

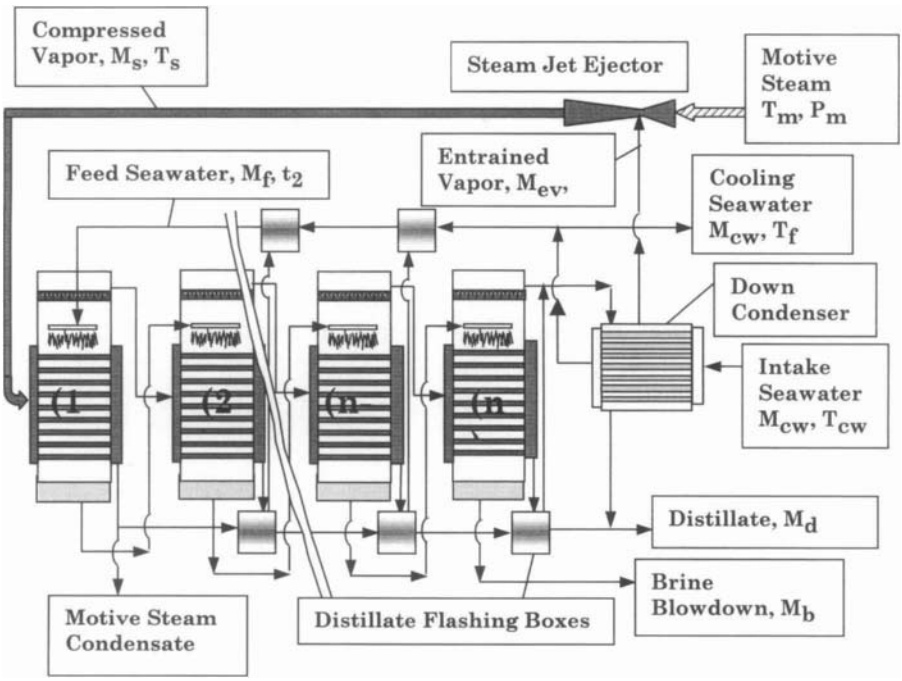

Fig. 12. Forward feed multiple effect thermal vapor compression.

5.2.1 *Process Modeling*

The mathematical model is divided into two parts; the first is for the MEE system and the second is for the steam jet ejector. Model equations and solution of the MEE system is given in the previous chapter. In addition, the steam jet ejector model is given in the previous section. Calculations of the MEE system variables are independent on the steam jet ejector equations. This includes temperature, flow rates, and concentration profiles as well as the heat transfer

area in the effects. However, the performance parameters of the MEE system are dependent on the characteristics of the steam jet ejector. Also, the design of the steam jet ejector is affected by the vapor temperature in the last effect of MEE and the specification of the steam temperature (compressed vapor) required for operating the MEE system. The performance parameters in the MEE system, which are affected by the design of the steam jet ejector, are the performance ratio, the specific heat transfer area, and the specific cooling water flow rate. The following sections include brief listing of the model equations for the MEE and the steam jet ejector and are followed solution of different case studies.

MEE Model

The simplified mathematical model of the MEE (discussed in the previous chapter) is used to calculate the following:

- Brine and distillate flow rates.
- Brine concentration.
- Effect temperature.
- Evaporator heat transfer area.

The model equations exclude the flash boxes and preheaters. The model includes the governing equation for the down condenser and its solution is made upon completion of the effect iterations and design of the steam jet ejector.

- Total mass balance

$$M_f = M_d + B_n \tag{41}$$

- Total salt balance

$$X_f M_f = X_n B_n \tag{42}$$

where B is the brine mass flow rate, M is the mass flow rate, X is the salt concentration, and the subscripts d, f, and n define the product water, feed seawater, and last effect.

- Distillate flow rate in the first effect

$$D_1 = M_d /(1 + \lambda_{v_1}/\lambda_{v_2} + ... + \lambda_1/ \lambda_{v_{n-1}} + \lambda_1/ \lambda_{v_n}) \tag{43}$$

- Distillate flow rate in effects 2 to n

$$D_n = D_1 \lambda_{v_1}/\lambda_{v_n} \tag{44}$$

- Total temperature drop across the effects

$$\Delta T = T_s - T_n \tag{45}$$

where D is the distillate flow rate, λ_v is the latent heat of formed vapor, and T_n are the temperatures of the motive steam and the vapor formed in the last effect.

- Temperature drop in the first effect

$$\Delta T_1 = \frac{\Delta T_t}{U_1 \sum_{i=1}^{n} \frac{1}{U_i}} \tag{46}$$

- Temperature drop in effects 2 to n

$$\Delta T_i = \Delta T_1 \, U_1/U_i \tag{47}$$

- Temperature of the first effect

$$T_1 = T_s - \Delta T_1 \tag{48}$$

- Temperature of effects 2 to n

$$T_i = T_{i-1} - \Delta T_1 \, U_1/U_i \tag{49}$$

- Brine flow rate in the first effect

$$B_1 = M_f - D_1 \tag{50}$$

- Brine flow rate in effects 2 to n

$$B_i = B_{i-1} - D_i \tag{51}$$

- Brine salt concentration in the first effect

$$X_1 = X_f \, M_f/B_1 \tag{52}$$

- Brine salt concentration in effects 2 to n

$$X_i = X_{i-1} \, B_{i-1}/B_i \tag{53}$$

- Heat transfer area in the first effect

$$A_1 = M_s \, \lambda_s / (U_1 \, (T_s - T_1)) = (D_1 \, \lambda_1 + M_f \, C_p \, (t_{f_2} - T_1)) / (U_1 \, (T_s - T_1)) \tag{54}$$

– Heat transfer area in effects 2 to n

$$A_i = D_i \lambda_i / (U_i (\Delta T_i - \Delta T_{loss})) \quad (55)$$

Performance Parameters

The performance ratio, PR, is defined as the flow rate ratio of distillate, M_d, and motive steam, M_m,

$$PR = M_d/M_m \quad (56)$$

The motive steam flow rate, M_m, is defined as the difference of the flow rates for the compressed vapor and the entrained vapor

$$M_m = M_s - M_{ev}$$

From Eq. 17

$$M_{ev} = M_m/Ra$$

The above two equations are simplified and an expression for the motive steam flow rate is obtained as a function of the compressed vapor flow rate

$$M_m = M_s/(1+1/Ra) \quad (57)$$

The compressed vapor flow rate is obtained from the thermal load for the first effect

$$M_s = (D_1 \lambda_{v1} + M_f Cp (T_1 - t_{f_2}))/ \lambda_s \quad (58)$$

where t_{f_2} is the seawater temperature leaving the last feed preheater.
The specific heat transfer area is

$$sA = \frac{\sum_{i=1}^{n} A_i + A_c}{M_d} \quad (59)$$

where A_i is the heat transfer area in effect i and A_c is the down condenser heat transfer area, which is obtained from

$$A_c = \frac{Q_c}{U_c (LMTD)_c} \tag{60}$$

The $(LMTD)_c$ is defined as:

$$(LMTD)_c = \frac{t_f - t_{cw}}{\ln \frac{T_n - t_{cw}}{T_n - t_f}} \tag{61}$$

The condenser thermal load

$$Q_c = (D_n - M_{ev})\, \lambda_{vn} \tag{62}$$

The specific cooling water flow rate

$$sM_{cw} = M_d / M_{cw} \tag{63}$$

The condenser energy balance,

$$(D_n - M_{ev})\, \lambda_{vn} = (M_f + M_{cw})\, Cp\, (t_f - t_{cw}) \tag{64}$$

where M_{cw}, is the cooling water flow rate.

Solution Procedure

Solution of the MEE-TVC model proceeds as follows:

- Solution of the overall material and salt balances, Eqs. 41 and 42.
- Iterative solution of the MEE model, Eqs. 43-55.
- Solution of the steam jet ejector model (Eq. 16 in Section 5.1).
- Evaluation of the performance parameters, Eqs. 56-64.

The following set of specifications is used in the above solution procedure:

- The seawater temperature, $T_{cw} = 25°C$.
- The feed water temperature leaving the last preheater, $T_{f_2} = T_1 - 5$.
- The seawater salinity, $X_f = 42000$ ppm.
- The salinity of the rejected brine, $X_b = 70000$ ppm.
- The range for top brine temperature, 55-100 °C.
- The range for the motive steam pressure, 250-1750 kPa.
- The range for the number of effects in MEE, 4-12 effects.
- The vapor temperature in the last effect, $T_n = 40$ °C.
- The thermodynamic losses in each effect, $\Delta T_i = 2$ °C.
- The heat capacity of all liquid streams, $C_p = 4.2$ kJ/kg °C.

- The overall heat transfer coefficient in the condenser, U_c = 1.75 kW/m^2 °C.
- The overall heat transfer coefficient in the first effect, U_e = 2.4 kW/m^2 °C; this value decreases by 5% in each subsequent effect.

5.2.2 Case Study

A four-effect MEE-TVC system is designed using the model and solution procedure discussed above. Specifications of the system parameters are given in the previous section. However, calculations are made at the following conditions:

- Compressed vapor temperature, T_s, 60 °C.
- Pressure of motive steam, P_m, 250 kPa.

For a total distillate flow rate, M_d, of 1 kg/s, intake seawater salinity, X_f, 42000 ppm, and rejected brine salinity of 70000 ppm, the resulting feed flow rate, M_f, and rejected brine from the last effect, B_4, are

$$M_f = X_b/(X_b - X_f) = 70000/(70000 - 42000) = 2.5 \text{ kg/s}$$

$$M_b = M_f - M_d = 2.5 - 1 = 1.5 \text{ kg/s}$$

The temperature drop across the effects, T_s–T_4, is equal to 60 – 40 = 20 °C. The overall heat transfer coefficients in effects 1 to 4 are specified and are assumed to remain constant throughout the iterations. The overall heat transfer coefficient in the first effect, U_1, is set equal to 2.4 kW/m^2 °C. Values in subsequent effects are obtained from

$$U_{i+1} = 0.95\ U_i$$

Values of the overall heat transfer coefficient in all effects are summarized in the following table

U_1	U_2	U_3	U_4
2.4	2.28	2.16	2.0577

The summation of the inverse for the overall heat transfer coefficients is required to calculate the temperature drop per effect. This summation is

$$\frac{1}{\sum_{i=1}^{6} U_i} = 1/U_1 + 1/U_2 + 1/U_3 + 1/U_4$$

$$= 1/2.4 + 1/2.28 + 1/2.16 + 1/2.0577 = 1.8029 \text{ m}^2\,^{\circ}\text{C/kW}$$

The temperature drop in the first effect is then calculated

$$\Delta T_1 = \frac{\Delta T_t}{U_1 \sum_{i=1}^{n} \frac{1}{U_i}} = \frac{20}{(2.4)(2.8529)} = 4.6221\ ^{\circ}\text{C}$$

The values of ΔT_i are calculated for effects 2 to 4

$\Delta T_2 = \Delta T_1\ (U_1/U_2) = (4.6221)(2.4)/(2.28) = 4.8654\ ^{\circ}\text{C}$

$\Delta T_3 = \Delta T_1\ (U_1/U_3) = (4.8654)(2.4)/(2.166) = 5.1215\ ^{\circ}\text{C}$

$\Delta T_4 = \Delta T_1\ (U_1/U_4) = (5.1215)(2.4)/(2.0577) = 5.391\ ^{\circ}\text{C}$

The following table summarizes the above values

ΔT_1	ΔT_2	ΔT_3	ΔT_4
4.6221	4.8654	5.1215	5.391

The temperature profile in effects 1 to 4 is then calculated

$T_1 = T_S - \Delta T_1 = 60 - 4.6221 = 55.3779\ ^{\circ}\text{C}$

$T_2 = T_1 - \Delta T_1\ (U_1/U_2) = 55.3779 - 4.6221\ (2.4/2.28) = 50.5\ ^{\circ}\text{C}$

$T_3 = T_2 - \Delta T_1\ (U_1/U_3) = 50.5125 - 4.6221\ (2.4/2.166) = 45.4\ ^{\circ}\text{C}$

To check the above values T_4 is calculated on

$T_4 = T_3 - \Delta T_1\ (U_1/U_4) = 45.391 - 4.6221\ (2.4/2.0577) = 40\ ^{\circ}\text{C}$

This value checks with the initial specification of 40 °C. The following table includes summary of calculated temperatures as well as the temperature of the motive steam.

T_S	T_1	T_2	T_3	T_4
60	55.3779	50.5125	45.3910	40

The latent heat values in all effects are calculated using the correlation given in the appendix

$\lambda_S = 2499.5698 - 2.204864\ T_s - 2.304x10^{-3}\ T_s^2$
$= 2499.5698 - 2.204864$ (Chapter 5 Multiple Effect Evaporation – Vapor
$= 2358.9$ kJ/kg

$\lambda_{V1} = 2499.5698 - 2.204864\ T_{V1} - 2.304x10^{-3}\ T_{V1}^2$
$= 2499.5698 - 2.204864\ (55.3779 - 2) - 2.304x10^{-3}\ (55.3779 - 2)^2$
$= 2375.3$ kJ/kg

$\lambda_{V2} = 2499.5698 - 2.204864\ T_{V2} - 2.304x10^{-3}\ T_{V2}^2$
$= 2499.5698 - 2.204864\ (50.5125 - 2) - 2.304x10^{-3}\ (50.5125 - 2)^2$
$= 2387.1$ kJ/kg

$\lambda_{V3} = 2499.5698 - 2.204864\ T_{V3} - 2.304x10^{-3}\ T_{V3}^2$
$= 2499.5698 - 2.204864\ (45.391 - 2) - 2.304x10^{-3}\ (45.391 - 2)^2$
$= 2399.5$ kJ/kg

$\lambda_{V4} = 2499.5698 - 2.204864\ T_{V4} - 2.304x10^{-3}\ T_{V4}^2$
$= 2499.5698 - 2.204864\ (40 - 2) - 2.304x10^{-3}\ (40 - 2)^2$
$= 2412.4$ kJ/kg

Summary of the latent heat values is given in the following table, which includes the latent heat of motive steam.

λ_S	λ_{V1}	λ_{V2}	λ_{V3}	λ_{V4}
2358.9	2375.3	2387.1	2399.5	2412.4

The flow rate profiles of the distillate and brine as well as the brine concentrations are calculated from Eqs. 3,4 and 10-13. The distillate flow rate in the first effect is calculated from Eq. 3

$D_1 = M_d\ /(\ 1 + \lambda_{V1}/\lambda_{V2} + \lambda_{V1}/\lambda_{V3} + \lambda_{V1}/\lambda_{V4})$
$= (1)/(1 + (2375.3/2387.1) + (2375.3/2399.5)$
$+ (2284.47/2412.4))$
$= 0.2519$ kg/s

Subsequently, the distillate flow rates in effects 2 to n are calculated

$D_2 = D_1 \lambda_{V_1}/\lambda_{V_2} = 0.1712\ (2375.3/2387.1) = 0.2507$ kg/s

$D_3 = D_1 \lambda_{V_1}/\lambda_{V_3} = 0.1712\ (2375.3/2399.5) = 0.2494$ kg/s

$D_4 = D_1 \lambda_{V_1}/\lambda_{V_4} = 0.1712\ (2375.3/2399.5) = 0.248$ kg/s

The brine flow rates are obtained from Eqs. 10 and 11

$B_1 = M_f - D_1 = 2.5 - 0.2519 = 2.2481$ kg/s

$B_2 = B_1 - D_2 = 2.2481 - 0.2507 = 1.9974$ kg/s

$B_3 = B_2 - D_3 = 1.9974 - 0.2494 = 1.748$ kg/s

$B_4 = B_3 - D_4 = 1.748 - 0.248 = 1.5$ kg/s

This value of B_4 checks with the initial material balance calculations. The salt concentration profile is calculated from Eqs. 12 and 13.

$X_1 = X_f M_f / B_1 = 42000\ (2.5/2.2481) = 46706.5078$ ppm

$X_2 = X_1 B_1/B_2 = 46706.5078\ (2.2481/1.9974) = 52567.9687$ ppm

$X_3 = X_2 B_2/B_3 = 52567.9687\ (1.9974/1.748) = 60067.2617$ ppm

$X_4 = X_3 B_3/B_4 = 60067.2617\ (1.748/1.5) = 70000$ ppm

The value of X_4 checks with the initial specification at 70,000 ppm. Summary for the values of distillate and brine flow rates and brine concentration are given in the following table.

Effect	1	2	3	4
D (kg/s)	0.2519	0.507	0.2494	0.248
B (kg/s)	2.2481	1.9974	1.748	1.5
X (ppm)	46706.5	52567.9	60067.2	70000

The heat transfer areas are calculated in effects 1 to 4. These values are calculated as follows:

$A_1 = (D_1 \lambda_{V_1} + M_f Cp\ (T_{f_2} - T_1))/(U_1(T_S - T_1))$

$= (0.2519)(2375.3) + (2.5)\ (4.2)\ (5))/(2.4(60 - 55.3779))$

$= 58.67\ m^2$

$A_2 = D_2\ \lambda_{v2}/(U_2(\Delta T_2 - \Delta T_{loss}))$
$= (0.2507)(2387.18)/(2.28(4.8654-2))$
$= 91.59\ m^2$

$A_3 = D_3\ \lambda_{v3}/(U_3(\Delta T_3 - \Delta T_{loss}))$
$= (0.2494)(2399.56)/(2.166(5.1215-2))$
$= 88.5\ m^2$

$A_4 = D_4\ \lambda_{v4}/(U_4(\Delta T_4 - \Delta T_{loss}))$
$= (0.248)(2412.45)/(2.0577(5.391-2))$
$= 85.757\ m^2$

The maximum difference in effect areas is equal to 32.9 m^2. Assuming an error criterion of less than 1 m^2 is required, therefore, a new iteration sequence has to be initiated. The second iteration starts with calculations of the new heat transfer area

$$A_m = \frac{\sum_{i=1}^{n} A_i}{n}$$
$= (58.675 + 91.5932 + 88.5045 + 85.7571)/4$
$= 324.529/4$
$= 81.13\ m^2$

A new profile for the temperature drop across the effects is then calculated

$\Delta T_1 = \Delta T_1\ (A_1/A_m) = (4.6221)(58.675)/(81.1324) = 3.3427\ ^oC$

$\Delta T_2 = \Delta T_2\ (A_2/A_m) = (4.8654)\ (91.5932)/(81.1324) = 5.4927\ ^oC$

$\Delta T_3 = \Delta T_3\ (A_3/A_m) = (5.1215)\ (88.5045)/(81.1324) = 5.5868\ ^oC$

$\Delta T_4 = \Delta T_4\ (A_4/A_m) = (5.391)\ (85.7571)/(81.1324) = 5.6983\ ^oC$

A new iteration is then taken, which starts with temperature profiles and continues to the convergence criteria part. The number of iterations executed to reach the above tolerance is 4. Summary of flow rates, concentrations, temperatures, and heat transfer areas in the last iteration are given in the following table

Effect	1	2	3	4
D (kg/s)	0.2518	0.2508	0.2498	0.2476
B (kg/s)	2.2482	1.9974	1.746	1.5
X (ppm)	46703	52567	60082	70000
T (°C)	56.54	52.9	49.07	40
A (m^2)	78.3	77.5	78.2	78.7

Determination of the entrainment ratio (Ra) requires calculations of the correction factors, PCF and TCF, or

$$PCF = 3x10^{-7} (P_m)^2 - 0.0009 (P_m) + 1.6101$$
$$= 3x10^{-7} (250)^2 - 0.0009 (250) + 1.6101$$
$$= 1.40385$$

$$TCF = 2x10^{-8} (T_{v_4})^2 - 0.0006 (T_{v_4}) + 1.0047$$
$$= 2x10^{-8} (38)^2 - 0.0006 (38) + 1.0047$$
$$= 0.9819$$

$$Ra = 0.296 \frac{(P_6)^{1.19}}{(P_7)^{1.04}} \left(\frac{P_m}{P_7}\right)^{0.015} \left(\frac{PCF}{TCF}\right)$$
$$= 0.296 \frac{(19.87)^{1.19}}{(6.527)^{1.04}} \left(\frac{250}{6.527}\right)^{0.015} \left(\frac{1.4038}{0.981}\right)$$
$$= 2.228$$

The above results should be checked against permissible ranges specified in the steam ejector model, where $Ra \leq 5$, $500 \geq T_m > 10$ °C, $3500 \geq P_m \geq 100$ kPa, and $(P_6/P_7) \geq 1.81$. The value of Ra is less than 5 and the ratio (P_6/P_7) is equal to 3.04 which is greater than 1.81. Also the values of T_m and P_m are within the specified range, where P_m is equal to 250 kPa and T_m is equal to 127.5 °C.

To obtain the performance ratio it is necessary to determine the flow rates of the motive steam, entrained vapor, and compressed vapor. The compressed vapor flow rate is given by

$$M_s = (D_1 \lambda_{v_1} / + C_p M_f (T_1 - T_{f_2})) / \lambda_s$$
$$= (0.2518)(2372.45) + 2.5) (4.2) (5)) / (2358.98)$$
$$= 0.2754 \text{ kg/s}$$

The motive steam flow rate is obtained from

$M_m = M_s/(1+1/Ra)$
$= 0.19$ kg/s

The entrained vapor flow rate is obtained from

$M_{ev} = M_s - M_m$
$= 0.275 - 0.19$
$= 0.08532$ kg/s

Since the total distillate flow rate is equal to 1 kg/s, then,

$PR = M_d/M_m = 1/0.19 = 5.26$

The condenser thermal load is calculated from

$Q_c = (D_4 - M_{ev})\,\lambda_{v4} = (0.2476 - 0.085329)\,(2412.46) = 391.47$ kW

The logarithmic mean temperature difference in the condenser is given by

$(LMTD)_c = (t_f - t_{cw})/Ln((T_4 - \Delta T_{loss} - t_{cw})/(T_4 - \Delta T_{loss} - t_f))$
$= (35\text{-}25)/Ln((40\text{-}2\text{-}25)/(40\text{-}2\text{-}35))$
$= 6.819\ ^oC$

The condenser heat transfer area in the condenser is then calculated from

$A_c = Q_c/(U_c\,(LMTD)_c) = 391.765/((1.75)(6.819)) = 32.79\ m^2$

The specific heat transfer area is calculated by the summing the heat transfer areas for the six evaporators and the condenser. This is

$$sA = \frac{\sum_{i=1}^{n} A_i + A_c}{M_d} = (312.96+32.79) = 345.76\ m^2$$

The cooling water flow rate is obtained from Eq. 29

$(D_4 - M_{ev})\,\lambda_{v4} = (M_f + M_{cw})\,Cp\,(t_f - t_{cw})$
$(0.2476\text{-}0.08532)(2412.45) = (2.5+M_{cw})\,(4.2)(35\text{-}25)$

which gives $M_{cw} = 6.819$ kg/s. The specific cooling water flow rate has the same value, since the total product flow rate is equal to 1 kg/s.

5.2.3 System Performance

Performance of the MEE-FF-TVC system together with the stand-alone MEE-FF system is shown in Figs. 13-15. The analysis is performed as a function of the number of effects and the heating steam temperature. As is shown performance ratio of the vapor compression system is higher, especially at low operating temperatures. The decrease in the performance ratio of the TVC system at higher temperatures is caused by the increase in the compression range. This is because the brine temperature in the last effect is kept constant in all calculations. Therefore, at higher temperature larger amount of motive steam is used to achieve the required compression range. This also affects the required amount of specific flow rate of cooling water. Results show the increase in the specific flow rate of cooling water for vapor compression system at higher operating temperatures and smaller number of effects. Increase in the system operating temperature increases the amount of motive steam, which increases the system thermal load and the required amount of cooling water per kg of distillate product.

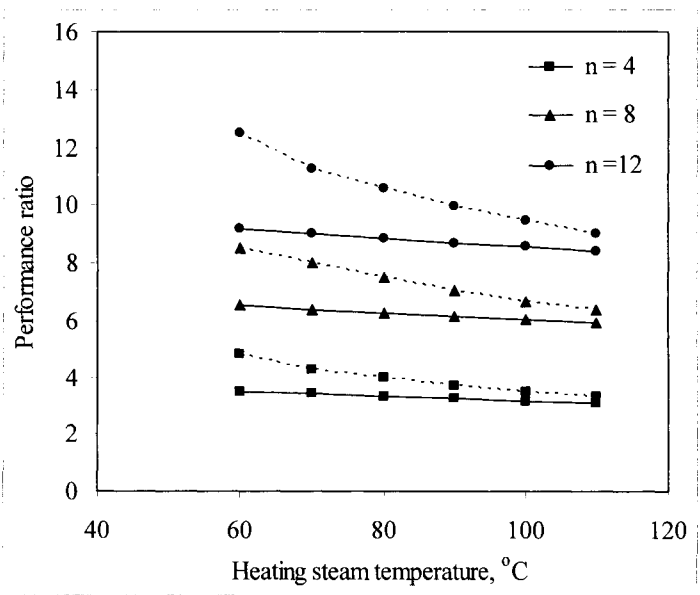

Fig. 13. Effect of heating steam temperature and the number of effects on the performance ratio of the MEE (—) and MEE-TVC (----) systems.

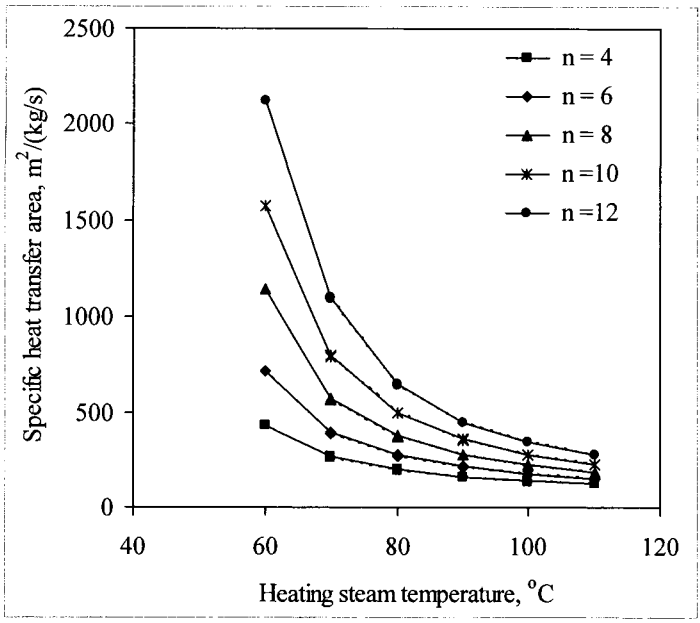

Fig. 14. Effect of heating steam temperature and the number of effects on the specific heat transfer area of the MEE (——) and MEE-TVC (----).

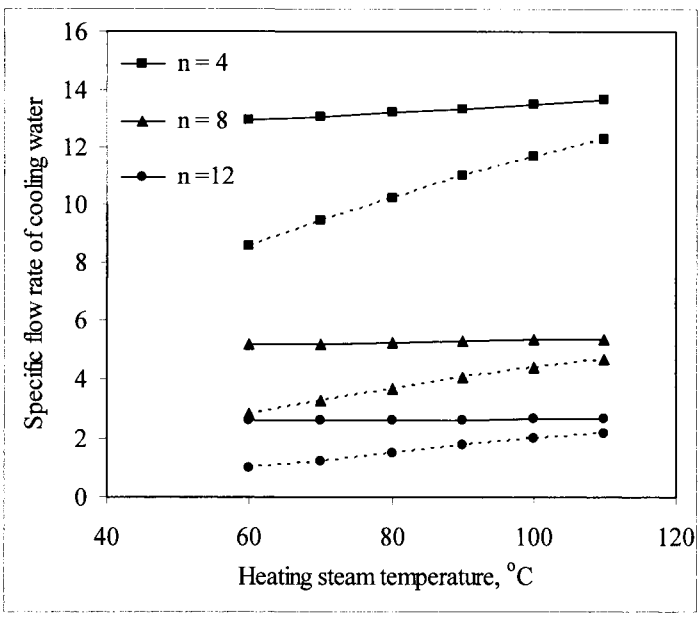

Fig. 15. Variation in specific flow rate of cooling water as a function of heating steam temperature and number of effects for MEE (——) and MEE-TVC (----).

Increase in the specific flow rate of cooling water at lower number of effects is caused by the increase in the amount of vapor generated per effect. Therefore, the amount of vapor generated in the last effect becomes larger and would require a larger amount of cooling water. It should be noted that the specific heat transfer area is slightly affected by the vapor compression process. This is because the effect temperatures remain the same for system operation with/without vapor compression. The main difference between the two systems comes in the heat transfer area for the down condenser, which is lower in the vapor compression mode due to vapor entrainment by the ejector.

5.2.4 Comparison of MEE and MEE-TVC

Performance characteristics of the MEE and MEE-TVC systems are compared for a four-effect system. Comparison includes performance ratio, specific heat transfer area, and specific cooling water flow rate. Results are summarized in the following Table. As is shown, the characteristics of the MEE-TVC out perform those for the MEE system; where

- The performance ratio is higher by 45%.
- The specific cooling water flow rate is lower by 41.8%.
- The condenser specific heat transfer area is lower by 34.4%.
- The total specific heat transfer area is lower by 4.75%.

Since, the characteristics of the MEE evaporators are identical in either configuration the same specific heat transfer area for the evaporators is obtained for both systems.

Process	MEE		MEE-TVC		MEE-TVC	
T_s	112.9	60.9	112.9	60.9	112.9	60.9
T_n	40	40	40	40	40	40
T_{cw_i}	25	25	25	25	25	25
T_{cw_o}	35	35	35	35	35	35
n	12	4	12	12	4	4
Power(1)	86.3	287.9	84.81	89.1	274.3	283.2
M_{cw}	4.47	14.2	4.11	2.2	8	12
A_c	16.37	39.5	15.34	15.8	36.2	37.5
sA	202.5	302.8	201.5	2119	280.5	428.7
Pr	8.67	2.52	9.2	12.5	3.3	4.8

(1) In kJ/kg and excluding the pumping power.

5.2.5 Summary

This section is focused on modeling and performance analysis of the forward feed multiple effect evaporation with thermal vapor compression. The analysis included a step-by-step calculation method for the MEE-TVC system, detailed mathematical model, performance as a function of the top brine temperature and the number of effects, and comparison against the stand-alone forward feed MEE system. Results show increase up to 50% in the thermal performance ratio and a similar decrease in the specific flow rate of cooling water. Operation of field units gives similar behavior.

Problems

Problem 1

A four effect parallel feed MEE-TVC system is shown in the attached figures. The system operates at the following conditions:

Temperature of the first effect = 58 °C
Temperature of the second effect = 54 °C,
Temperature of the third effect = 50 °C
Temperature of the fourth effect = 46 °C
Temperature of heating steam = 63 °C
Motive steam flow rate = 6.88 kg/s, Motive steam pressure = 15 bar
Entrained vapor flow rate = 8 kg/s
Amount of vapor formed in the first effect = 14 kg/s
Amount of vapor formed in the second effect = 13.2 kg/s
Amount of vapor formed in the third effect = 13.2 kg/s
Amount of vapor formed in the fourth effect = 14 kg/s
Flow rate of product water = 52.6 kg/s

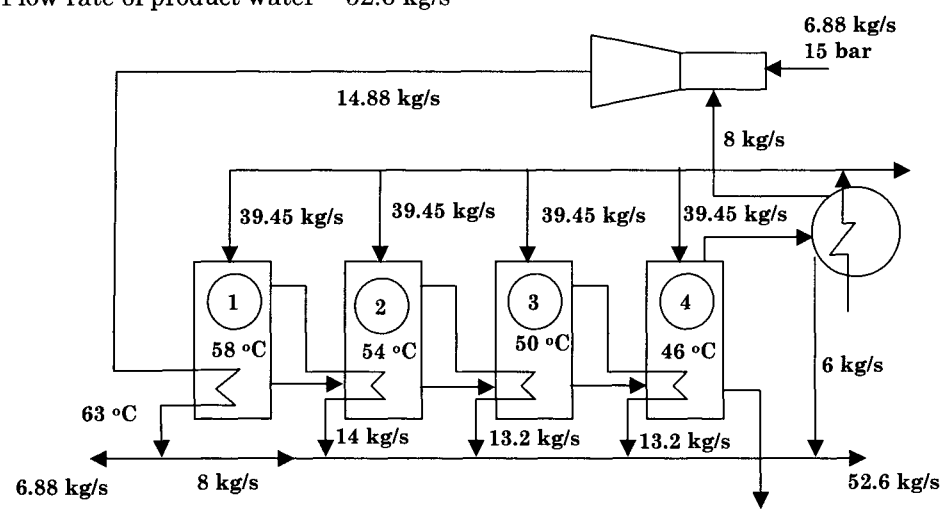

Calculate the following
- Plant performance ratio
- Specific heat transfer area
- Mass flow rate of rejected cooling water
- Pressure of the motive steam

Problem 2

A four effect forward feed MEE-TVC system operates at the following conditions:

Plant capacity = 1000 m^3/d
Motive steam pressure = 250 kPa
Ejector area ratio = 50
Temperature of vapor in the last effect = 65 °C
Temperature of feed seawater = 40 °C
Feed seawater salinity = 45000 ppm

The overall heat transfer coefficient is given by

$$U = 3.25 + 0.05 (T - 60)$$

Where U is in kW/m^2 °C and T is in °C

Calculate the following
- Plant performance ratio
- Flow rates of cooling seawater and motive steam

Problem 3

A Three effect forward feed MEE-TVC system operates at the following conditions:

Plant capacity = 500 m^3/d
Temperature of feed seawater = 20 °C
Feed seawater salinity = 42000 ppm
Salinity of brine blow down = 70000 ppm
Temperature of vapor in the last effect = 45 °C
Motive steam pressure = 250 kPa
Ejector area ratio = 50
Temperature of compressed heating steam = 80 °C

The overall heat transfer coefficients in the three effects are equal to

$U_1 = 3.123$ kW/m^2 °C

$U_2 = 1.987$ kW/m^2 °C

$U_3 = 1.136$ kW/m^2 ^oC

Calculate the following

- Plant performance ratio
- The specific heat transfer area
- The specific flow rate of cooling water

5.3 *Forward Feed Multiple Effect Evaporation with Mechanical Vapor Compression*

A schematic diagram for the MEE-MVC system is shown in Fig. 16, where it has a similar set for the MEE configuration except for removal of the down condenser and addition of the feed preheaters, a flashing box for the first effect, and the mechanical compressor. The compressor unit operates on the entire vapor formed in the last effect, where it is compressed to the desired pressure and superheat temperature. This is necessary to take into consideration the lower amount of vapor formed in the last effect in comparison with that formed in the first effect. Routing the entire vapor formed in the last effect to compressor results in elimination of the down condenser. However, to maintain high thermal efficiency for the process plate preheaters are used to increase the temperature of the feed seawater from (T_{cw}) to (T_f). This is achieved by heat recovery from the brine blowdown and the distillate product streams in two separate feed preheaters.

5.3.1 *System Model*

Elements forming the model of the forward feed multiple effect evaporation are a combination of the mathematical model for the stand-alone forward feed system together with the mathematical model for the mechanical vapor compressor. Therefore, it is advisable to review elements of both models. The forward feed model is given in section 5.2 and the model on mechanical vapor compression is given in the chapter on single effect systems.

5.3.2 *System Performance*

Performance of the forward feed multiple effect system is shown in Figs. 17-18. Performance results are obtained for the specific power consumption and the specific heat transfer area. Results are presented as a function of the brine blowdown temperature, the temperature difference of the brine between the first and last effects, and the number of effects.

Fig. 17 shows variations in the specific power consumption for both systems, where it decreases at higher operating temperature and lower temperature differences of the brine. At higher operating temperatures, the specific volume of the vapor decreases, which reduces the power consumed for vapor compression. On the other hand, larger temperature differences of the saturation temperature of the compressed vapor and the brine blowdown result in increase in the compression range, which increases the power consumed for vapor compression. The specific power consumption for the both systems and the above set of parameters varies between low values close to 6 kWh/m^3 and higher values close to 14 kWh/m^3, which are consistent with literature data.

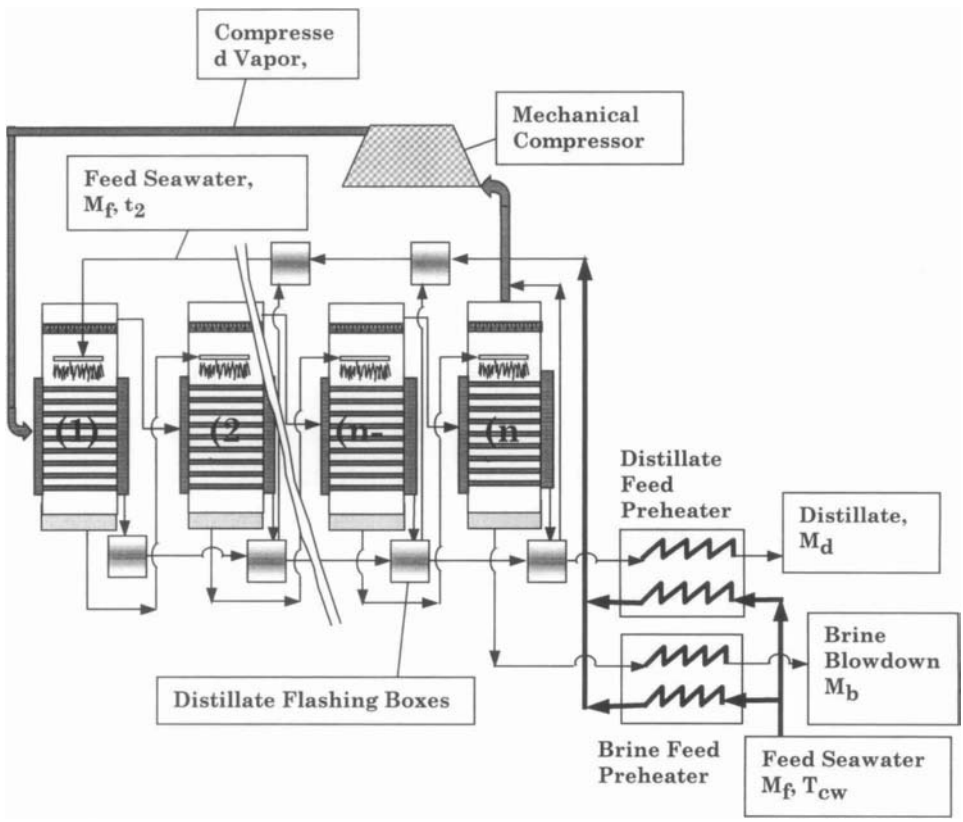

Fig. 16. Forward feed multiple effect evaporation with mechanical vapor compression

Figure 18 shows that the specific heat transfer has stronger dependence on the temperature drop per stage rather than the top brine temperature. The temperature drop per stage is affected by the number of effects and the temperature difference between the first and last effects. On the other hand, increase in the system temperature has smaller effect on the specific heat transfer area. Increase in the system temperature has a limited effect on the heat transfer coefficient and the heat transfer area.

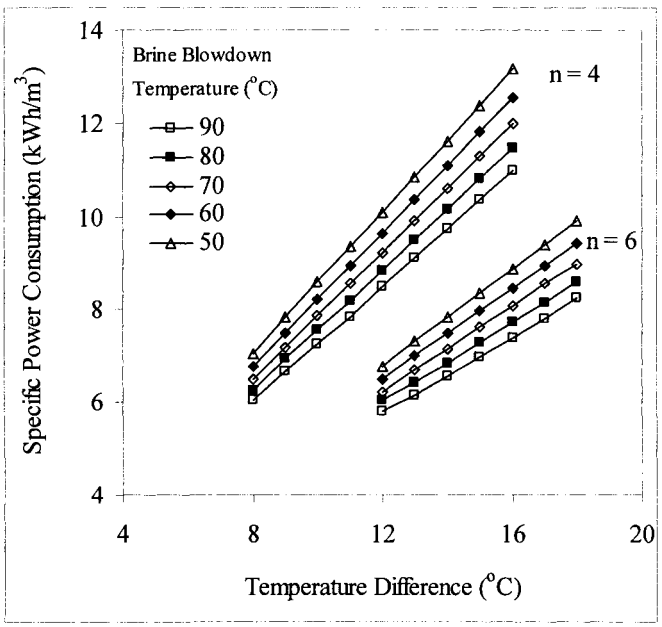

Fig. 17. Variation in specific power consumption for the forward feed multiple effect with mechanical vapor compression.

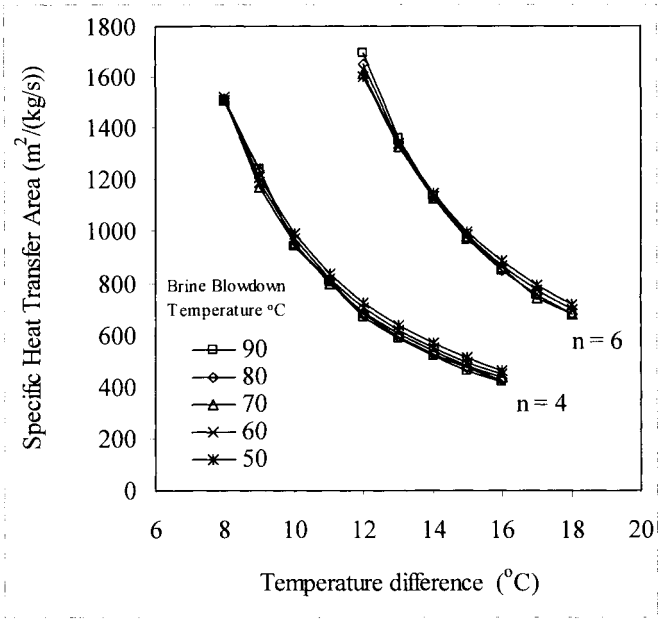

Fig. 18. Variation in specific heat transfer area for the forward feed multiple effect with mechanical vapor compression.

5.4 Forward Feed Multiple Effect Evaporation with Adsorption Vapor Compression

The MEE-ADS includes two beds for vapor adsorption and desorption, Fig. 19. Similar to MEE-MVC, the system does not include a down condenser. Therefore, the intake seawater is heated in two plate preheaters against the brine blowdown and the distillate product. Operation of the adsorption/desorption heat pump is transient and it involves simultaneous condensation/adsorption of vapor formed in the last effect/flash box into the adsorption bed and evaporation/desorption of heating steam from the desorption bed. In each bed zeolite solid is used as the adsorption/desorption medium. Adsorption proceeds at an equilibrium temperature corresponding to the vapor temperature in the last effect; while, while desorption proceeds at an equilibrium temperature corresponding to the heating steam temperature in the first effect. External heating/cooling sources are used to assist the adsorption/desorption processes. Cooling water is used to remove the latent heat of condensation from the adsorption bed, while, motive steam is used to add the latent heat of evaporation for the desorption bed. The desorption process reaches an equilibrium dry condition as most of the adsorbed water is released as vapor. Similarly, the wet equilibrium condition in the adsorption bed is reached as the

bed solid phase becomes saturated with water. Upon completion of the adsorption/desorption processes, the external cooling/heating sources are disengaged. Subsequently, the thermal fluid circulates between the two beds to remove the sensible heat from the dry bed into the wet bed. This heat exchange process increases the temperature of the cold/wet bed to a higher value close to the required desorption temperature. Similarly, the temperature of dry/hot bed is reduced to a temperature that allows the start of the adsorption process. However, it should be stressed that reaching conditions required to start the adsorption/desorption process requires additional cooling/heating by the cooling water and the motive steam.

As discussed in the previous section, the mathematical model for this system is a combination of the forward feed multiple effect system, which is given in section 5.2, and the adsorption heat pump model, which is given in chapter 3.

Performance analysis of this system is limited to evaluation of the thermal performance ratio and comparison against the stand-alone system. This is because variations in other system parameters are similar to those of the stand-alone system. Variations in the thermal performance ratio as a function of the heating steam temperature and number of effects is shown in Fig. 20. As is shown, the thermal performance ratio increases by more than 100% over the stand-alone system, especially, at high temperatures. For example, the thermal performance ratio for the 12 effect system is equal to 24 at a heating steam temperature of 115 ^{o}C. On the other hand, the thermal performance ratio of the stand-alone system it is equal to a value of 8. It should be noted that the thermal performance ratio for the system increases with the increase of the system temperature. This is because of the decrease in the latent heat of desorption at higher temperatures.

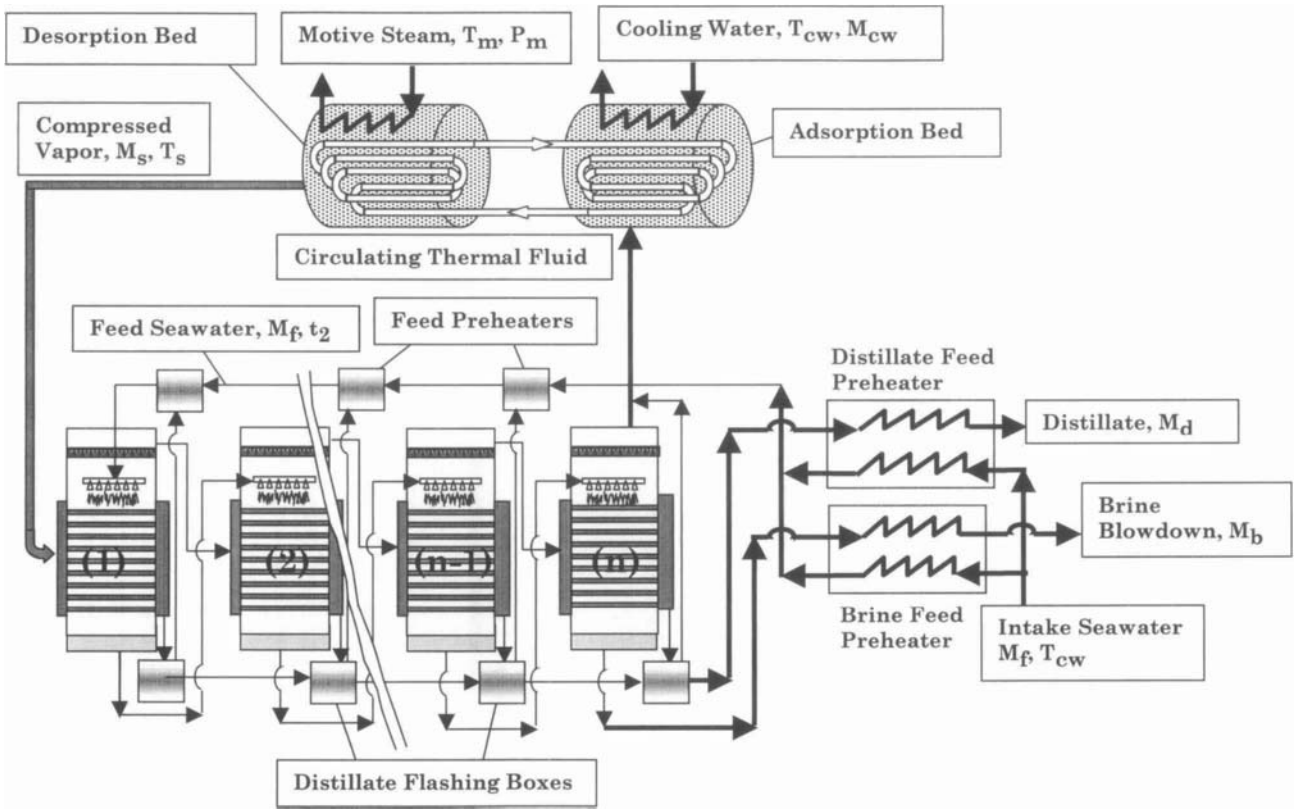

Fig. 19. Forward feed multiple effect evaporation with adsorption vapor compression

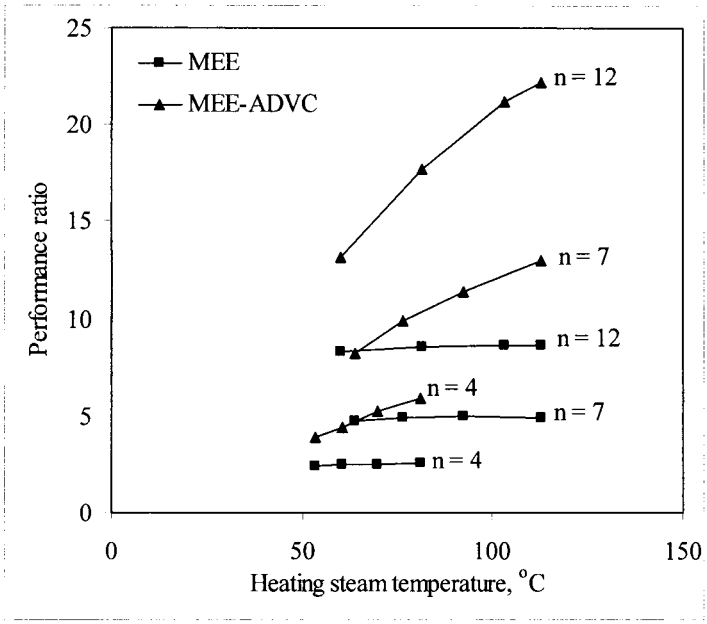

Fig. 20. Variation in the performance ratio for the forward feed multiple effect with adsorption vapor compression.

5.5 *Forward Feed Multiple Effect Evaporation with Absorption Vapor Compression*

The MEE-ABS system, shown in Fig. 21, includes evaporation effects, flashing boxes, feed preheaters, down condenser, stripping and absorption beds containing lithium bromide water solution (LiBr-H_2O). As is shown, part of the vapor formed in the last effect/flashing box is condensed in the down condenser, where it releases its latent heat to the feed seawater. The remaining part of the vapor flows through the absorption bed where it is absorbed the concentrated (LiBr-H_2O) solution. The absorption process is exothermic, where the feed seawater absorbs the released heat. This result in heating of the feed seawater to the saturation temperature and formation of a small amount of saturated vapor. The dilute LiBr-H2O solution is feed to the generator or stripper, where heat added by the motive steam results in water evaporation and increase in the solution concentration. The concentrated LiBr solution is pumped back to the absorption bed. The vapors formed in the generator and the absorber are combined together and are used to drive the evaporation effect number (1).

The mathematical model for this system is a combination of the forward feed multiple effect system, which is given in section 5.2, and the adsorption heat pump model, which is given in chapter 3. Similarly, the system performance, except for the thermal performance ratio, is similar to the stand-alone system. Variations in the thermal performance ratio as a function of the heating steam temperature and number of effects is shown in Fig. 22. As is shown, the thermal performance ratio increases by more than 100% over the stand-alone system, especially, at high temperatures. For example, the thermal performance ratio for the 12 effect system is equal to 27 at a heating steam temperature of 115 ^{o}C. On the other hand, the thermal performance ratio of the stand-alone system it is equal to a value of 8. It should be noted that the thermal performance ratio for the system increases with the increase of the system temperature. This is because of the decrease in the latent heat of desorption at higher temperatures.

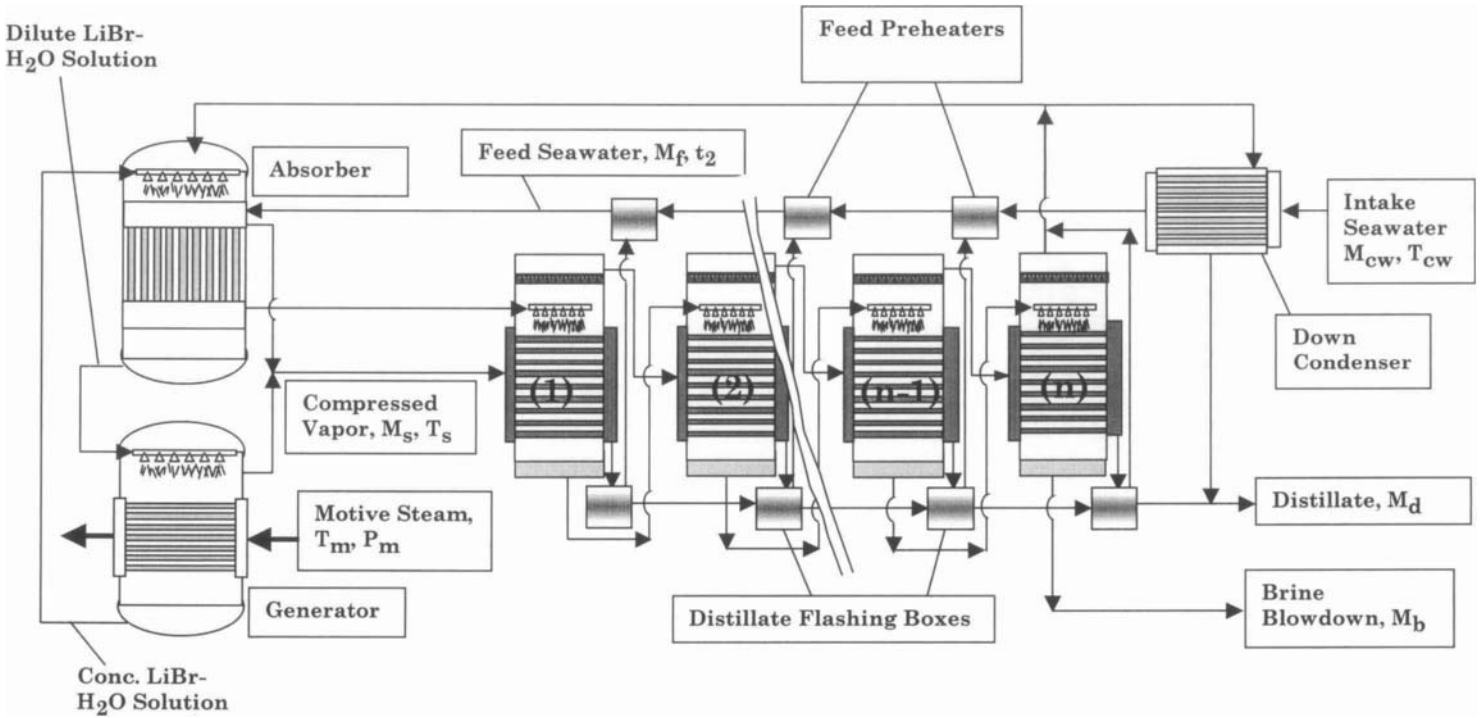

Fig. 21. Forward feed multiple effect evaporation with absorption vapor compression

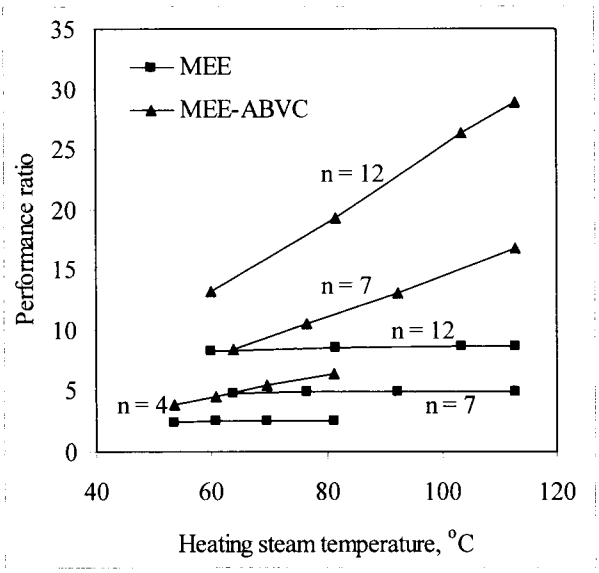

Fig. 22. Variation in the thermal performance ratio for the forward feed multiple effect evaporation with absorption vapor compression.

5.6 Summary

Four configurations are investigated for the forward feed MEE desalination system. The systems include combinations with thermal, mechanical, adsorption, and absorption vapor compression. The combined systems make efficient use of the characteristics of the MEE system and the combined heat pump. In the combined MEE-ADS and MEE-ABS systems, the first and last effects of the MEE system replace the condenser and evaporator units of the heat pump. This selection reduces the equipment cost of the heat pump. The combined system, also, allows for heating of utility water, which has a great value in industrial applications. These features are not found in the MEE, the MEE-MVC, and the MEE-TVC systems.

Mathematical models are developed for the proposed configurations. Results show large increase in the performance ratio of the hybrid MEE systems against that of the MEE configuration. In addition, results show the possibility of operating the hybrid systems at high steam temperatures. This was made possible by utilizing two steam ejectors in the MEE-TVC system and by using heat pumps in the MEE-ABS and MEE-ADS systems. In addition, results for the MEE-MVC system show the possibility of operation at high steam temperatures.

This is a major advantage for all systems, where at high steam temperatures the evaporator area in all effects is drastically reduced. This in turn will decrease considerably the construction cost of the MEE system.

In summary the following conclusions are made

- High increase in the performance ratio in the hybrid systems in comparison with conventional MEE.
- Increase of the top brine temperature reduces dramatically the required specific heat transfer area for all configurations.
- The MEE-MVC requires no cooling water, however, use of auxiliary heat is necessary to drive the first effect.
- The MEE-TVC requires less cooling water than conventional MEE.
- The MEE-ABS and MEE-ADS generates hot utility water, which can be used in other applications.
- Predictions of all models show very good agreement with industrial practice, i.e., performance ratio, power consumption, specific heat transfer area, and specific cooling water flow rate.
- Hybrid MEE-heat pump systems have great potential to replace conventional MSF (predominant in current desalination practice) in the near future.